

# Learning Temporally Extended Skills in Continuous Domains as Symbolic Actions for Planning

Jan Achterhold      Markus Krimmel      Joerg Stueckler

Embodied Vision Group, Max Planck Institute for Intelligent Systems, Tübingen, Germany  
 {jan.achterhold,markus.krimmel,joerg.stueckler}@tuebingen.mpg.de

**Abstract:** Problems which require both long-horizon planning and continuous control capabilities pose significant challenges to existing reinforcement learning agents. In this paper we introduce a novel hierarchical reinforcement learning agent which links temporally extended skills for continuous control with a forward model in a symbolic discrete abstraction of the environment’s state for planning. We term our agent SEADS for Symbolic Effect-Aware Diverse Skills. We formulate an objective and corresponding algorithm which leads to unsupervised learning of a diverse set of skills through intrinsic motivation given a known state abstraction. The skills are jointly learned with the symbolic forward model which captures the effect of skill execution in the state abstraction. After training, we can leverage the skills as symbolic actions using the forward model for long-horizon planning and subsequently execute the plan using the learned continuous-action control skills. The proposed algorithm learns skills and forward models that can be used to solve complex tasks which require both continuous control and long-horizon planning capabilities with high success rate. It compares favorably with other flat and hierarchical reinforcement learning baseline agents and is successfully demonstrated with a real robot.<sup>1</sup>

**Keywords:** temporally extended skill learning, hierarchical reinforcement learning, diverse skill learning

## 1 Introduction

Reinforcement learning agents have been applied to difficult continuous control and discrete planning problems such as the DeepMind Control Suite [1], StarCraft II [2], or Go [3] in recent years. Despite this tremendous success, tasks which require both continuous control capabilities and long-horizon discrete planning still pose significant challenges to reinforcement learning agents [4]. An exemplary class of environments which require both continuous-action control and long-horizon planning are *physically embedded games* as introduced by [4]. In these environments, a board game is embedded into a physical manipulation setting. A move in the board game can only be executed indirectly through controlling a physical manipulator such as a robotic arm. We simplify the setting of [4] and introduce physically embedded *single-player* board games which do not require to model the effect of an opponent. Our experiments support the findings of [4] that these environments are challenging to solve for existing flat and hierarchical reinforcement learning agents. In this paper, we propose a novel hierarchical reinforcement learning agent for such environments which learns skills and their effects in a known symbolic abstraction of the environment.

As a concrete example for a proposed embedded single-player board game we refer to the *Lights-OutJaco* environment (see Fig. 1). Pushing a field on the *LightsOut* board toggles the illumination state (*on* or *off*) of the field and its non-diagonal neighboring fields. A field on the board can only be pushed by the end effector of the *Jaco* robotic arm. The goal is to reach a board state in which all fields are *off*. The above example also showcases the two concepts of *state* and *action* abstraction in decision making [5]. A state abstraction function  $\Phi(s_t)$  only retains information in  $s_t$  which is relevant for a particular decision making task. In the *LightsOut* example, to decide which move to

<sup>1</sup>Project website (including video) is available at <https://seads.is.tue.mpg.de/>

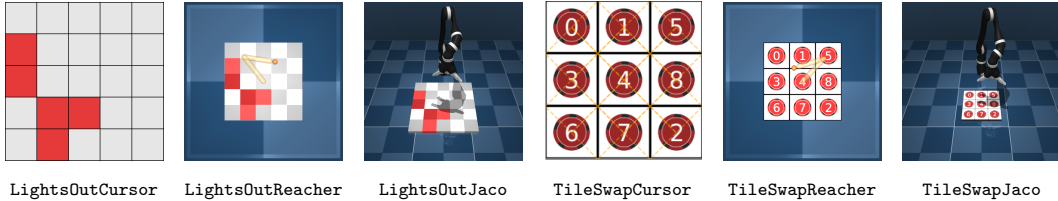


Figure 1: *LightsOut* (with on (red) and off (gray) fields) and *TileSwap* (fields in a rhombus are swapped if pushed inside) board games embedded into physical manipulation settings. A move in the board game can only indirectly be executed through controlling a manipulator.

perform next (i.e., which field to push), only the illumination state of the board is relevant. A *move* can be considered an *action abstraction*: A skill, i.e. high-level action (e.g., push top-left field), comprises a sequence of low-level actions required to control the robotic manipulator.

We introduce a two-layer hierarchical agent which assumes a discrete state abstraction  $z_t = \Phi(s_t) \in \mathcal{Z}$  to be known and observable in the environment, which we in the following refer to as *symbolic observation*. In our approach, we assume that state abstractions can be defined manually for the environment. For *LightsOut*, the symbolic observation corresponds to the state of each field (on/off). We provide the state abstraction as prior knowledge about the environment and assume that skills induce changes of the abstract state. Our approach then learns a diverse set of skills for the given state abstraction as action abstractions and a corresponding forward model which predicts the effects of skills on abstract states. In board games, these abstract actions relate to *moves*. We jointly learn the predictive forward model  $f$  and *skill policies*  $\pi(a | s_t, k)$  for low-level control through an objective which maximizes the number of symbolic states reachable from any state of the environment (diversity) and the predictability of the effect of skill execution. Please see Fig. 2 for an illustration of the introduced temporal and symbolic hierarchy. The forward model  $f$  can be leveraged to plan a sequence of skills to reach a particular state of the board (e.g., all fields off), i.e. to solve tasks.

We evaluate our approach using two single-player board games in environments with varying complexity in continuous control. We demonstrate that our agent learns skill policies and forward models suitable for solving the associated tasks with high success rate and compares favorably with other flat and hierarchical reinforcement learning baseline agents. We also demonstrate our agent playing *LightsOut* with a real robot.

In summary, we contribute the following: (1) We formulate a novel reinforcement learning algorithm which, based on a state abstraction of the environment and an information-theoretic objective, jointly learns a diverse set of continuous-action skills and a forward model capturing the temporally abstracted effect of skill execution in symbolic states. (2) We demonstrate the superiority of our approach compared to other flat and hierarchical baseline agents in solving complex physically-embedded single-player games, requiring high-level planning and continuous control capabilities. We will publish the source code of our proposed method together with the final version of this paper.

## 2 Related work

**Diverse skill learning and skill discovery.** Discovering general skills to control the environment through exploration without task-specific supervision is a fundamental challenge in reinforcement learning research. DIAYN [6] formulates skill discovery using an information-theoretic objective as reward. The agent learns a skill-conditioned policy for which it receives reward if the target states can be well predicted from the skill. VALOR [7] proposes to condition the skill prediction model on the complete trajectory of visited states. Warde-Farley et al. [8] train a goal-conditioned policy to reach diverse states in the environment. Variational Intrinsic Control [9] proposes to use an information-theoretic objective to learn a set of skills which can be identified from their initial and target states. Relative Variational Intrinsic Control [10] seeks to learn skills relative to their start state, aiming to avoid skill representations that merely tile the state space into goal state regions. Both approaches do not learn a forward model on the effect of skill execution like our approach. Sharma et al. [11] propose a model-based RL approach (DADS) which learns a set of diverse skills and their dynamics models using mutual-information-based exploration. While DADS learns skill dynamics as immediate behavior  $q(s_{t+1}|s_t, k)$ , we learn a transition model on the effect of skills  $q(z_T|z_0, k)$  in a symbolic abstraction, thereby featuring temporal abstraction.

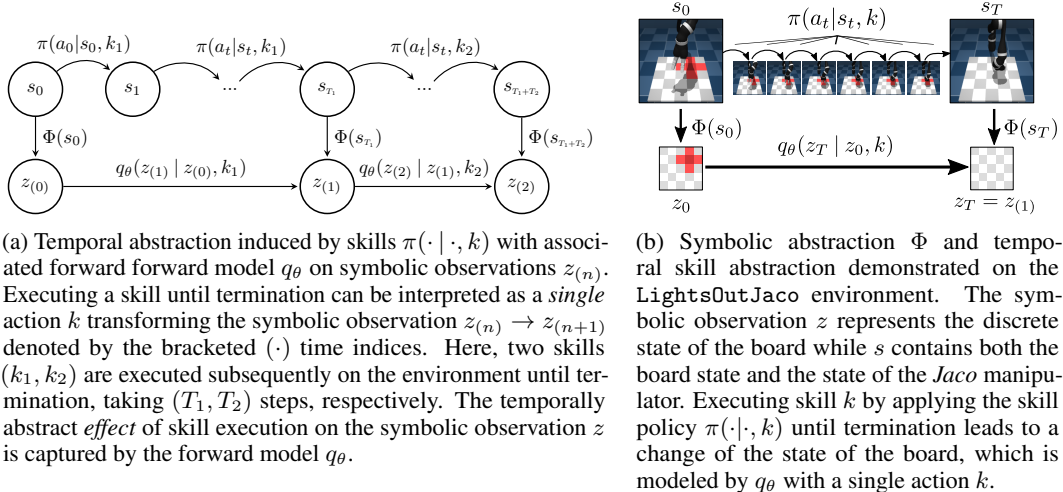


Figure 2: We aim to learn skills with associated policies  $\pi(a_t | s_t, k)$  which, if executed until termination, lead to diverse and predictable (by the forward model  $q_\theta$ ) transitions in a symbolic abstraction  $z = \Phi(s)$  of the state  $s$ . (a) depicts the relation of states, symbolic observations, policy and symbolic forward model. (b) shows an example of skill execution on the `LightsOutJaco` environment.

**Hierarchical reinforcement learning.** Hierarchical reinforcement learning can overcome sparse reward settings and time extended tasks by breaking the task down into subtasks. Some approaches such as methods based on MAXQ [12, 13] assume prior knowledge on the task-subtask decomposition. In SAC-X [14], auxiliary tasks assist the agent in learning sparse reward tasks and hierarchical learning involves choosing between tasks. Florensa, Duan, and Abbeel [15] propose to learn a span of skills using stochastic neural networks for representing policies. The policies are trained in a task-agnostic way using a measure of skill diversity based on mutual information. Specific tasks are then tackled by training an RL agent based on the discovered skills. Feudal approaches [16] such as HIRO [17] and HAC [18] train a high-level policy to provide subgoals for a low-level policy. In our method, we impose that a discrete state-action representation exists in which learned skills are discrete actions, and train the discrete forward model and the continuous skill policies jointly.

Several approaches to hierarchical reinforcement learning are based on the options framework [19] which learns policies for temporally extended actions in a two-layer hierarchy. Learning in the options framework is usually driven by task rewards. Recent works extend the framework to continuous spaces and discovery of options (e.g. [20, 21]). HiPPO [22] develop an approximate policy gradient method for hierarchies of actions. HIDIO [23] learns task-agnostic options using a measure of diversity of the skills. In our approach, we also learn task-agnostic (for the given state abstraction) hierarchical representations using a measure of intrinsic motivation. However, an important difference is that we do not learn high-level policies over options using task rewards, but learn a skill-conditional forward model suitable for planning to reach a symbolic goal state. Jointly, continuous policies are learned which implement the skills.

**Representation learning for symbolic planning.** Some research has been devoted to learning representations for symbolic planning. Konidaris, Kaelbling, and Lozano-Perez [24] propose a method for acquiring a symbolic planning domain from a set of low-level options which implement abstract symbolic actions. In [25] the approach is extended to learning symbolic representations for families of SMDPs which describe options in a variety of tasks. Our approach learns action abstractions as a set of diverse skills given a known state abstraction and a termination condition which requires abstract actions to change abstract states. Toro Icarte et al. [26] learn structure and transition models of finite state machines through reinforcement learning. Ugur and Piater [27] acquire symbolic forward models for a predefined low-level action repertoire in a robotic manipulation context. Other approaches such as DeepSym [28] or LatPlan [29] learn mappings of images to symbolic states and learn action-conditional forward models. In LatPlan [29] symbolic state-action representations are learned from image observations of discrete abstract actions (such as moving tiles in a tile puzzle to their discrete locations) which already encode the planning problem. Our approach learns a diverse

set of skills (i.e. discrete actions) based on an information-theoretic intrinsic reward and learns the symbolic forward model concurrently. Differently, in our approach low-level actions are continuous.

### 3 Method

Our goal is to learn a hierarchical reinforcement learning agent which (i) enables high-level, temporally abstract planning to reach a particular goal configuration of the environment (as given by a symbolic observation) and (ii) features continuous control policies to execute the high-level plan. Let  $\mathcal{S}, \mathcal{A}$  denote the state and action space of an environment, respectively. In general, by  $\mathcal{Z} = \{0, 1\}^D$  we denote the space of discrete symbolic environment observations  $z \in \mathcal{Z}$  and assume the existence of a state abstraction  $\Phi : \mathcal{S} \rightarrow \mathcal{Z}$ . The dimensionality of the symbolic observation  $D$  is environment-dependent. For the *LightsOutJaco* environment, the state  $s = [q, \dot{q}, z] \in \mathcal{S}$  contains the robot arms' joint positions and velocities  $(q, \dot{q})$  and a binary representation of the board  $z \in \{0, 1\}^{5 \times 5}$ . The action space  $\mathcal{A}$  is equivalent to the action space of the robotic manipulator. In the *LightsOutJaco* example, it contains the target velocity of all actuable joints.

We equip our agent with symbolic planning and plan execution capabilities through two components: First, the forward model  $\hat{z} = f(z, k) = \operatorname{argmax}_{z'} q_\theta(z' | z, k)$  allows to *enumerate* all possible symbolic successor states  $\hat{z}$  of the current symbolic state  $z$  by iterating over the discrete variable  $k \in \mathcal{K} = \{1, \dots, K\}$ . This allows for node expansion in symbolic planners. Second, a family of discretely indexed policies  $\pi : \mathcal{A} \times \mathcal{S} \times \mathcal{K} \rightarrow \mathbb{R}$ ,  $a_t \sim \pi(a_t | s_t, k)$  aims to steer the environment into a target state  $s_T$  for which it holds that  $\Phi(s_T) = \hat{z}$ , given that  $\Phi(s_0) = z$  and  $\hat{z} = \operatorname{argmax}_{z'} q_\theta(z' | z, k)$  (see Fig. 2). We can relate this discretely indexed family of policies to a set of  $K$  options [19]. An option is formally defined as a triple  $o_k = (I_k, \beta_k, \pi_k)$  where  $I_k \subseteq \mathcal{S}$  is the set of states in which option  $k$  is applicable,  $\beta_k : \mathcal{S} \times \mathcal{S} \rightarrow [0, 1]$ ,  $\beta_k(s_0, s_t)$  parametrizes a Bernoulli probability of termination in state  $s_t$  when starting in  $s_0$  and  $\pi_k(a | s_t) : \mathcal{S} \rightarrow \Delta(\mathcal{A})$  is the option policy on the action space  $\mathcal{A}$ . We will refer to the option policy as *skill policy* in the following. We assume that all options are applicable in all states, i.e.,  $I_k = \mathcal{S}$ . An option terminates if the symbolic state has changed between  $s_0$  and  $s_t$ , i.e.,  $\beta_k(s_0, s_t) = \mathbf{1}[\Phi(s_0) \neq \Phi(s_t)]$ . We define the operator *apply* as  $s_T = \operatorname{apply}(E, \pi, s_0, k)$  which applies the skill policy  $\pi(a_t | s_t, k)$  until termination on environment  $E$  starting from initial state  $s_0$  and returns the terminal state  $s_T$ . We also introduce a bracketed time notation which abstracts the effect of skill execution from the number of steps  $T$  taken until termination  $s_{(n)} = \operatorname{apply}(E, \pi, s_{(n-1)}, k)$  with  $n \in \mathbb{N}_0$  (see Fig. 2a). The *apply* operator can thus be rewritten as  $s_{(1)} = \operatorname{apply}(E, \pi, s_{(0)}, k)$  with  $s_{(0)} = s_0, s_{(1)} = s_T$ .

The symbolic forward model  $q_\theta(z_T | z_0, k)$  aims to capture the relation of  $z_0, k$  and  $z_T$  for  $s_T = \operatorname{apply}(E, \pi, s_0, k)$  with  $z_0 = \Phi(s_0), z_T = \Phi(s_T)$ . The model factorizes<sup>2</sup> over the symbolic observation as  $q_\theta(z_T | k, z_0) = \prod_{d=1}^D q_\theta([z_T]_d | k, z_0) = \prod_{d=1}^D \operatorname{Bernoulli}([\alpha_T]_d)$ . The Bernoulli probabilities  $\alpha_T : \mathcal{Z} \times \mathcal{K} \rightarrow (0, 1)^D$  are predicted by a neural component. We use a multilayer perceptron (MLP)  $f_\theta$  which predicts the probability  $p_{\text{flip}}$  of binary variables in  $z_0$  to toggle  $p_{\text{flip}} = f_\theta(z_0, k)$ .

**Objective** For any state  $s_0 \in \mathcal{S}$  with associated symbolic state  $z_0 = \Phi(s_0)$  we aim to learn  $K$  skills  $\pi(a | s_t, k)$  which maximize the diversity in the set of reachable successor states  $\{z_T^k = \Phi(\operatorname{apply}(E, \pi, s_0, k)) | k \in \mathcal{K}\}$ . Jointly, we aim to model the effect of skill execution with the forward model  $q_\theta(z_T | z_0, k)$ . Inspired by Variational Intrinsic Control [9] we take an information-theoretic perspective and maximize the mutual information  $\mathcal{I}(z_T, k | z_0)$  between the skill index  $k$  and the symbolic observation  $z_T$  at skill termination given the symbolic observation  $z_0$  at skill initiation, i.e.,  $\max \mathcal{I}(z_T, k | z_0) = \max H(z_T | z_0) - H(z_T | z_0, k)$ . The intuition behind this objective function is that we encourage the agent to (i) reach a diverse set of terminal observations  $z_T$  from an initial observation  $z_0$  (by maximizing the conditional entropy  $H(z_T | z_0)$ ) and (ii) behave predictably such that the terminal observation  $z_T$  is ideally fully determined by the initial observation  $z_0$  and skill index  $k$  (by minimizing  $H(z_T | z_0, k)$ ).

We reformulate the objective as an expectation over tuples  $(s_0, k, s_T)$  by employing the mapping function  $\Phi$  as  $\mathcal{I}(z_T, k | z_0) = \mathbb{E}_{(s_0, k, s_T) \sim P} \left[ \log \frac{p(z_T | z_0, k)}{p(z_T | z_0)} \right]$  with  $z_T := \Phi(s_T), z_0 := \Phi(s_0)$  and replay buffer  $P$ . Similar to [11] we derive a lower bound on the mutual information, which is maximized through the interplay of a reinforcement learning problem and maximum likelihood

<sup>2</sup>The index operator  $[x]_i$  returns the  $i^{\text{th}}$  element of vector  $x$ .

estimation. To this end, we first introduce a variational approximation  $q_\theta(z_T | z_0, k)$  to the transition probability  $p(z_T | z_0, k)$ , which we model by a neural component. We decompose

$$\mathcal{I}(z_T, k | z_0) = \mathbb{E}_{(s_0, k, s_T) \sim P} \left[ \log \frac{q_\theta(z_T | z_0, k)}{p(z_T | z_0)} \right] + \underbrace{\mathbb{E}_{(s_0, k, s_T) \sim P} \left[ \log \frac{p(z_T | z_0, k)}{q_\theta(z_T | z_0, k)} \right]}_{\approx \text{D}_{\text{KL}}(p(z_T | z_0, k) || q_\theta(z_T | z_0, k))}$$

giving rise to the lower bound  $\mathcal{I}(z_T, k | z_0) \geq \mathbb{E}_{(s_0, k, s_T) \sim P} \left[ \log \frac{q_\theta(z_T | z_0, k)}{p(z_T | z_0)} \right]$  whose maximization can be interpreted as a sparse-reward reinforcement learning problem with reward  $\hat{R}_T(k) = \log \frac{q_\theta(z_T | z_0, k)}{p(z_T | z_0)}$ . We approximate  $p(z_T | z_0)$  as  $p(z_T | z_0) \approx \sum_{k'} q_\theta(z_T | z_0, k') p(k' | z_0)$  and assume  $k$  uniformly distributed and independent of  $z_0$ , i.e.  $p(k' | z_0) = \frac{1}{K}$ . This yields a tractable reward

$$R_T(k) = \log \frac{q_\theta(z_T | z_0, k)}{\sum_{k'} q_\theta(z_T | z_0, k')} + \log K. \quad (1)$$

In section 3 we describe modifications we apply to the intrinsic reward  $R_T$  which improve the performance of our proposed algorithm. To tighten the lower bound, the KL divergence term in eq. 1 has to be minimized. Minimizing the KL divergence term corresponds to "training" the symbolic forward model  $q_\theta$  by maximum likelihood estimation of the parameter  $\theta$ .

**Training procedure** In each epoch of training, we first collect skill trajectories on the environment using the skill policy  $\pi$ . For each episode  $i \in \{1, \dots, N\}$  we reset the environment and obtain an initial state  $s_0^i$ . Next, we uniformly sample skills  $k^i \sim \text{Uniform}\{1, \dots, K\}$ . By iteratively applying the skill policy  $\pi(\cdot | \cdot, k^i)$  we obtain resulting states  $s_0^i \dots s_{T_i}^i$  and actions  $a_0^i \dots a_{T_i-1}^i$ . A skill rollout terminates either if an environment-dependent step-limit is reached or when a change in the symbolic observation  $z_t \neq z_0$  is observed. We append the rollouts to a limited-size buffer  $\mathcal{B}$ . In each training epoch we sample two sets of episodes  $\mathcal{S}_{\text{RL}}, \mathcal{S}_{\text{FM}}$  from the buffer for training the policy  $\pi$  and symbolic forward model  $q_\theta$ . Both episode sets are relabelled as described in Sec. 3. Let  $i \in \{1, \dots, M\}$  now refer to the episode index in the set  $\mathcal{S}_{\text{RL}}$ . From  $\mathcal{S}_{\text{RL}}$  we sample transition tuples  $([s_t^i, k^i], [s_{t+1}^i, k^i], a_t^i, r_{t+1}^i(k^i))$  which are used to update the policy  $\pi$  using the soft actor-critic (SAC) algorithm [30]. To condition the policy on skill  $k$  we concatenate  $k$  to the state  $s$  as denoted by  $[\cdot, \cdot]$ . We set the intrinsic reward to zero  $r_{t+1}^i = 0$  except for the last transition in an episode ( $t+1 = T_i$ ) in which  $r_{t+1}^i(k^i) = R(k^i)$ . From the episodes in  $\mathcal{S}_{\text{FM}}$  we form tuples  $(z_0^i = \Phi(s_0^i), k^i, z_{T_i}^i = \Phi(s_{T_i}^i))$  which are used to train the symbolic forward model using gradient descent.

**Relabelling** Early in training, the symbolic transitions caused by skill executions mismatch the predictions of the symbolic forward model. We can in *hindsight* increase the match between skill transitions and forward model by replacing the actual  $k^i$  which was used to collect the episode  $i$  by a different  $k_*^i$  in all transition tuples  $([s_t^i, k_*^i], [s_{t+1}^i, k_*^i], a_t^i, r_{t+1}^i(k_*^i))$  and  $(z_0^i, k_*^i, z_{T_i}^i)$  of episode  $i$ . In particular, we aim to replace  $k^i$  by  $k_*^i$  which has highest probability  $k_*^i = \max_k q_\theta(k | z_T, z_0)$ . However, this may lead to an unbalanced distribution over  $k_*^i$  after relabelling which is no longer uniform. To this end, we introduce a constrained relabelling scheme as follows. We consider a set of episodes indexed by  $i \in \{1, \dots, N\}$  and compute skill log-probabilities for each episode which we denote by  $Q_k^i = \log q_\theta(k | z_0^i, z_{T_i}^i)$  where  $q_\theta(k | z_0^i, z_{T_i}^i) = \frac{q_\theta(z_{T_i}^i, | z_0^i, k)}{\sum_{k'} q_\theta(z_{T_i}^i, | z_0^i, k')}$ . We find a relabeled skill for each episode  $(k_*^1, \dots, k_*^N)$  which maximizes the scoring  $\max_{(k_*^1, \dots, k_*^N)} \sum_i Q_{k_*^i}^i$  under the constraint that the counts of re-assigned skills  $(k_*^1, \dots, k_*^N)$  and original skills  $(k^1, \dots, k^N)$  match, i.e.<sup>3</sup>  $\#_{i=1}^N [k_*^i = k] = \#_{i=1}^N [k^i = k] \quad \forall k \in \{1, \dots, K\}$  which is to ensure that after relabelling no skill is over- or underrepresented. This problem can be formulated as a linear sum assignment problem which we solve using the Hungarian method [31, 32]. While we pass all episodes in  $\mathcal{S}_{\text{FM}}$  to the relabelling module, only a subset (50%) of episodes in  $\mathcal{S}_{\text{RL}}$  can potentially be relabeled to retain negative examples for the SAC agent. Relabelling experience in hindsight to improve sample efficiency is a common approach in goal-conditioned [33] and hierarchical [18] reinforcement learning.

**Reward improvements** The reward in equation 1 can be denoted as  $R(k) = \log q_\theta(k | z_0, z_T) + \log K$ . For numerical stability, we define a lower bounded term  $\bar{Q}_k = \text{clip}(\log q_\theta(k | z_0, z_T), \min =$

<sup>3</sup>The count operator  $\#[\cdot]$  counts the number of positive (true) evaluations of its argument in square brackets.

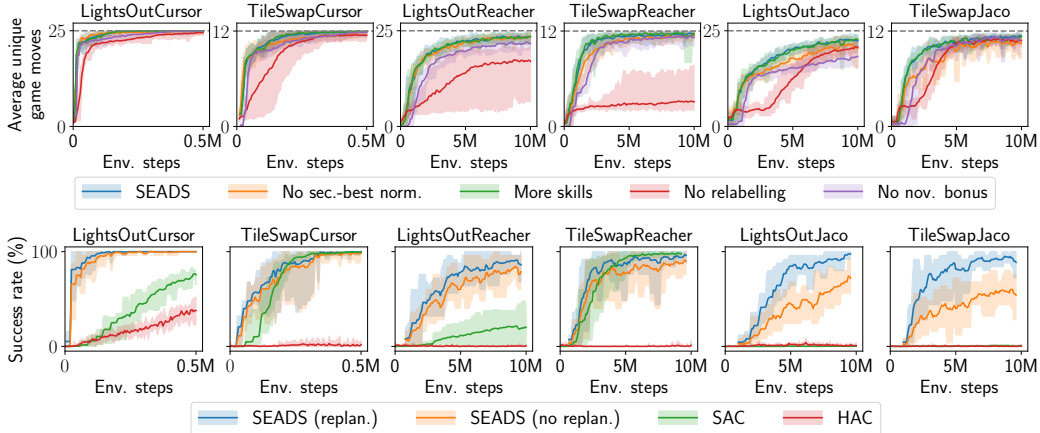


Figure 3: Top row: Number of learned unique game moves for ablations of SEADS (see sec. 4 for details). Bottom row: Success rate of the proposed SEADS agent and baseline methods on *LightsOut*, *TileSwap* games embedded in *Cursor*, *Reacher*, *Jaco* manipulation environments. SEADS performs comparably or outperforms the baselines on all tasks (see sec. 4 for details). The solid line depicts the mean, shaded area min. and max. of 10 independently trained agents

$-2 \log(K)$  and write  $R^0(k) = \bar{Q}_k + \log K$ . In our experiments, we observed that occasionally the agent is stuck in a local minimum in which (i) the learned skills are not unique, i.e., two or more skills  $k \in \mathcal{K}$  cause the same symbolic transition  $z_0 \rightarrow z_T$ . In addition, (ii), occasionally, not all possible symbolic transitions are discovered by the agent. To tackle (i) we reinforce the policy  $\pi$  with a positive reward if and only if no other skill  $k'$  better fits the symbolic transition ( $z_0 \rightarrow z_T$ ) generated by  $\text{apply}(E, \pi, s_0, k)$ , i.e.,  $R^{\text{norm}}(k) = \bar{Q}_k - \text{top2}_{k'} \bar{Q}_{k'}$ , which we call **second-best normalization**. The operator  $\text{top2}_{k'}$  selects the second-highest value of its argument for  $k' \in \mathcal{K}$ . We define  $R^{\text{base}}(k) = R^{\text{norm}}(k)$  except for the "No second-best norm." ablation where  $R^{\text{base}}(k) = R^0(k)$ . To improve (ii) the agent obtains a **novelty bonus** for transitions ( $z_0 \rightarrow z_T$ ) which are not modeled by the symbolic forward model for *any*  $k'$  by  $R(k) = R^{\text{base}}(k) - \max_{k'} \log q_\theta(z_T | z_0, k')$ .

**Planning and skill execution** A task is presented to our agent as an initial state of the environment  $s_0$  with associated symbolic observation  $z_0$  and a symbolic goal  $z^*$ . First, we leverage our learned symbolic forward model  $q_\theta$  to plan a sequence of skills  $k_1, \dots, k_N$  from  $z_0$  to  $z^*$  using breadth-first search (BFS). We use the mode of the distribution over  $z'$  for node expansion in BFS:  $\text{successor}_{q_\theta}(z, k) = \text{argmax}_{z' \in \mathcal{Z}} q_\theta(z' | z, k)$ . After planning, the sequence of skills  $[k_1, \dots, k_N]$  is iteratively applied to the environment through  $s_{(n)} = \text{apply}(E, \pi, s_{(n-1)}, k_n)$ . Inaccuracies of skill execution (leading to different symbolic observations than predicted) can be coped with by replanning after each skill execution. Both single-outcome (mode) determinisation and replanning are common approaches to probabilistic planning [34].

**Further details** on training and task execution with SEADS can be found in sec. S.5.

## 4 Experiments

We evaluate our proposed agent on a set of physically-embedded game environments. We follow ideas from [4] but consider single-player games which in principle enable full control over the environment without the existence of an opponent. We chose *LightsOut* and *TileSwap* as board games which are embedded in a physical manipulation scenario with *Cursor*, *Reacher* or *Jaco* manipulators (see Fig. 1). The *LightsOut* game (see Figure 1) consists of a  $5 \times 5$  board of fields. Each field has a binary illumination state of *on* or *off*. By pushing a field, its illumination state and the state of the (non-diagonally) adjacent fields toggles. At the beginning of the game, the player is presented a board where some fields are on and the others are off. The task of the player is to determine a set of fields to push to obtain a board where all fields are off. The symbolic observation in all *LightsOut* environments represents the illumination state of all 25 fields on the board  $\mathcal{Z} = \{0, 1\}^{5 \times 5}$ . In *TileSwap* (see Fig. 1) a  $3 \times 3$  board is covered by chips numbered from 0 to 8 (each field contains exactly one chip). Initially, the chips are randomly assigned to fields. Two chips can be swapped

if they are placed on (non-diagonally) adjacent fields. The game is successfully finished after a number of swap operations if the chips are placed on the board in ascending order. In all *TileSwap* environments the symbolic observation represents whether the  $i$ -th chip is located on the  $j$ -th field  $\mathcal{Z} = \{0, 1\}^{9 \times 9}$ . To ensure feasibility, we apply a number of random moves (pushes/swaps) to the goal board configuration of the respective game. We quantify the difficulty of a particular board configuration by the number of moves required to solve the game. We ensure disjointness of board configurations used for training and testing through a hashing algorithm (see sec. S.9).

In our proposed environments, performing a board game move is only possible through a robotic manipulator. A board game move ("push" in *LightsOut*, "swap" in *TileSwap*) is triggered by the manipulator's end effector touching a particular position on the board. We use three manipulators of different complexity (see Fig. 1). The *Cursor* manipulator can be navigated on the 2D game board by commanding  $x$  and  $y$  displacements. The board coordinates are  $x, y \in [0, 1]$ , the maximum displacement per timestep is  $\Delta x, \Delta y = 0.2$ . A third action triggers a push (*LightsOut*) or swap (*TileSwap*) at the current position of the cursor. The *Reacher* [1] manipulator consists of a two-link arm with two rotary joints. The position of the end effector in the 2D plane can be controlled by external torques applied to the two rotary joints. As for the *Cursor* manipulator an additional action triggers a game move at the current end effector coordinates. The *Jaco* manipulator [35] is a 9-DoF robotic arm whose joints are velocity-controlled at 10Hz. It has an end-effector with three "fingers" which can touch the underlying board to trigger game moves. By combining the games of *LightsOut* and *TileSwap* with the *Cursor*, *Reacher* and *Jaco* manipulators we obtain six environments. As step limit for skill execution we set 10 steps on *Cursor* and 50 steps in *Reacher* and *Jaco* environments.

With our experiments we aim at answering the following research questions: **R1:** How many distinct skills are learned by SEADS? Does SEADS learn all 25 (12) possible moves in *LightsOut* (*TileSwap*) reliably? **R2:** How do our design choices contribute to the performance of SEADS? **R3:** How well does SEADS perform in solving the posed tasks in comparison to other flat and hierarchical reinforcement learning approaches? **R4:** Can our SEADS also be trained and applied on a real robot?

**Skill learning evaluation** To address **R1** we investigate how many distinct skills are learned by SEADS. If not all possible moves within the board games are learned as skills (25 for *LightsOut*, 12 for *TileSwap*), some initial configurations are unsolvable for the agent, negatively impacting task performance. To count the number of learned skills we apply each skill  $k \in \{1, \dots, K\}$  on a fixed initial state  $s_0$  of the environment  $E$  until termination (i.e.,  $\text{apply}(E, s_0, \pi, k)$ ). Among these  $K$  skill executions we count the number of unique game moves being triggered. We report the average number of unique game moves for  $N = 100$  distinct initial states  $s_0$ . See sec. S.2 for a visualization of learned skills.

On the *Cursor* environments SEADS detects all possible game moves (avg. approx. 24.9 of 25 possible in *LightsOutCursor*, 12 of 12 in *TileSwapCursor*). For *Reacher* almost all moves are found (23.4/11.5). In the *Jaco* environments some moves are missing occasionally (22.4/11.4). We demonstrate superior performance compared to a baseline skill discovery method (Variational Intrinsic Control, Gregor, Rezende, and Wierstra [9]) in sec. S.8. We substantiate our agent design through an ablation study (**R2**) in which we compare the number of unique skills (game moves) detected for variants of SEADS (see Fig. 3). In a first study, we remove single parts from our agent to quantify their impact on performance. This includes training SEADS without the proposed *relabelling*, *second-best normalization* and *novelty bonus*. We found all of these innovations to be important for the performance of SEADS, with the difference to the full SEADS agent being most prominent in the *LightsOutJaco* environment. Over-estimating the number of skills required in case where the exact number of skills is unknown does not harm the performance of SEADS (*more skills* ablation with  $K = 30$  for *LightsOut*,  $K = 15$  for *TileSwap*). We present a detailed analysis in sec. S.4.

**Task performance evaluation** To evaluate the task performance of our agent and baseline agents (**R3**) we initialize the environments such that the underlying board game requires at maximum 5 moves (pushes in *LightsOut*, swaps in *TileSwap*) to be solved. We evaluate each agent on 20 examples for each number of moves in  $\{1, \dots, 5\}$  required to solve the game. We consider a task to be successfully solved if the target board configuration was reached (all fields *off* in *LightsOut*, ordered fields in *TileSwap*). For SEADS we additionally count tasks as "failed" if planning exceeds a wall time limit of 60 seconds. We evaluate both planning variants with and without replanning. As an instance of a flat (non-hierarchical) agent we evaluate the performance of Soft Actor-Critic (SAC, Haarnoja

et al. [30]). The SAC agent receives the full environment state  $s \in \mathcal{S}$  which includes the symbolic observation (board state). It obtains a reward of 1 if it successfully solved the game and 0 otherwise. In contrast to the Soft Actor-Critic agent the SEADS agent leverages the decomposition of state  $s \in \mathcal{S}$  and symbolic observation  $z \in \mathcal{Z}$ . For a fair comparison to a hierarchical agent, we consider Hierarchical Actor-Critic (HAC, Levy et al. [18]), which, similar to SEADS, can also leverage the decomposition of  $s$  and  $z$ . HAC consists of a multi-level hierarchy of policies. We employ a two-level hierarchy in which the high-level policy sets *symbolic* subgoals  $z \in \mathcal{Z}$  to the low-level policy, thereby leveraging the access to the symbolic observation. We refer to sec. S.6 (SAC) and sec. S.7 (HAC) for implementation and training details. Fig. 3 visualizes the performance of SEADS and the baselines. On all environments SEADS performs similar or outperforms the baselines, with the performance difference being most pronounced on the *Jaco* environments on which SAC and HAC do not make any progress. On the cursor environments SEADS achieves a success rate of 100% after  $5 \cdot 10^5$  environment steps. On the remaining environments, the average success rate (with replanning) is 86% (*LightsOutReacher*), 96% (*TileSwapReacher*), 97.6% (*LightsOutJaco*), 88.8% (*TileSwapJaco*) after  $10^7$  steps.

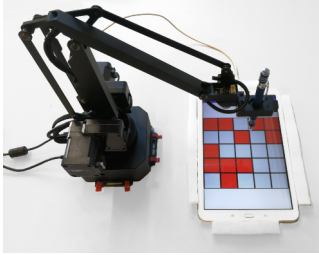


Figure 4: Robotic arm (uArm Swift Pro) interacting with a LightsOut game running on an Android tablet.

**Robot experiment** In order to evaluate the applicability of our approach on a real-world robotic system (R4) we set up a testbed with a uArm Swift Pro robotic arm which can interact with a tablet using a capacitive pen (see Fig. 4). The SEADS agent commands a position  $(x, y) \in [0, 1]^2$  (covering the tablet’s screen) to push to the arm, which then executes the push. The board state is communicated to the agent through the tablet’s USB interface. We manually reset the board *once* at the beginning of training, and do not interfere in the further process. After 5000 environment interactions (corresponding to  $\approx 7.5$  hours total training time) we evaluated the SEADS agent’s performance on 100 board configurations (20 per solution depth in  $\{1, \dots, 5\}$ ) and found all of them to be successfully solved by the agent. We refer to sec. S.3 for details.

## 5 Assumptions and Limitations

Our approach assumes that the state abstraction is known and the symbolic observation  $z$  is provided by the environment. Also, we assume that the continuous state is fully observable. Learning the state abstraction too is an interesting direction for future research. The breadth-first search planner we use for planning on the symbolic level exhibits scaling issues for large solution depths; e.g., for LightsOut it exceeds a 5-minute threshold for solution depths (number of initial board perturbations)  $\geq 9$ . In future work, more efficient heuristic or probabilistic planners could be explored. In the more complex environments (*Reacher*, *Jaco*) we observe our agent to not learn all possible skills reliably, in particular for skills for which no transitions exist in the replay buffer. In future work one could integrate additional exploration objectives which incentivize to visit unseen regions of the state space.

## 6 Conclusion

We present an agent which, in an unsupervised fashion, learns diverse skills in complex physically embedded board game environments which relate to *moves* in the particular games. We provide a state abstraction from continuous states to symbolic states as prior information which we assume observable to the agent. Additionally, we assume that skills lead to changes in the symbolic state. The jointly learned forward model captures the temporally extended *effects* of skill execution. We leverage this forward model to plan over a sequence of skills (moves) to execute in order to solve a particular task in the environment, i.e., bring the game board to a desired state. We demonstrate that with this formulation we can solve complex physically embedded games with high success rate and that our approach compares favorably with other flat and hierarchical reinforcement learning algorithms. We also demonstrate our approach on a real robot. Our approach provides an unsupervised learning alternative to prescribing the action abstraction and pretraining each skill individually before learning a forward model from skill executions. In future research, our approach could be combined with state abstraction learning to leverage its full potential.



## Acknowledgments

This work has been supported by Cyber Valley and the Max Planck Society. The authors thank the International Max Planck Research School for Intelligent Systems (IMPRS-IS) for supporting Jan Achterhold.

## References

- [1] Y. Tassa et al. “DeepMind Control Suite”. In: *ArXiv e-prints* (Jan. 2018). arXiv: 1801.00690 [cs.AI].
- [2] Oriol Vinyals et al. “Grandmaster level in StarCraft II using multi-agent reinforcement learning”. In: *Nat.* 575.7782 (2019), pp. 350–354. DOI: 10.1038/s41586-019-1724-z. URL: <https://doi.org/10.1038/s41586-019-1724-z>.
- [3] David Silver et al. “Mastering the Game of Go with Deep Neural Networks and Tree Search”. In: *Nature* 529.7587 (Jan. 2016), pp. 484–489. ISSN: 0028-0836. DOI: 10.1038/nature16961.
- [4] Mehdi Mirza et al. “Physically Embedded Planning Problems: New Challenges for Reinforcement Learning”. In: *CoRR* abs/2009.05524 (2020). arXiv: 2009.05524. URL: <https://arxiv.org/abs/2009.05524>.
- [5] George Konidaris. “On the necessity of abstraction”. In: *Current Opinion in Behavioral Sciences* 29 (2019). Artificial Intelligence, pp. 1–7. ISSN: 2352-1546. DOI: <https://doi.org/10.1016/j.cobeha.2018.11.005>.
- [6] Benjamin Eysenbach et al. “Diversity is All You Need: Learning Skills without a Reward Function”. In: *7th International Conference on Learning Representations, ICLR 2019, New Orleans, LA, USA, May 6-9, 2019*. OpenReview.net, 2019. URL: <https://openreview.net/forum?id=SJx63jRqFm>.
- [7] Joshua Achiam et al. “Variational Option Discovery Algorithms”. In: *CoRR* abs/1807.10299 (2018). arXiv: 1807.10299. URL: <http://arxiv.org/abs/1807.10299>.
- [8] David Warde-Farley et al. “Unsupervised Control Through Non-Parametric Discriminative Rewards”. In: *7th International Conference on Learning Representations (ICLR)*. 2019. URL: <https://openreview.net/forum?id=r1eVMnA9K7>.
- [9] Karol Gregor, Danilo Jimenez Rezende, and Daan Wierstra. “Variational Intrinsic Control”. In: *International Conference on Learning Representations (ICLR), Workshop Track Proceedings*. OpenReview.net, 2017. URL: <https://openreview.net/forum?id=Skc-Fo4Yg>.
- [10] Kate Baumli et al. “Relative Variational Intrinsic Control”. In: *AAAI Conference on Artificial Intelligence (AAAI)*. AAAI Press, 2021, pp. 6732–6740. URL: <https://ojs.aaai.org/index.php/AAAI/article/view/16832>.
- [11] Archit Sharma et al. “Dynamics-Aware Unsupervised Discovery of Skills”. In: *8th International Conference on Learning Representations, ICLR 2020, Addis Ababa, Ethiopia, April 26-30, 2020*. OpenReview.net, 2020. URL: <https://openreview.net/forum?id=HJgLZR4KvH>.
- [12] Thomas G. Dietterich. “Hierarchical Reinforcement Learning with the MAXQ Value Function Decomposition”. In: *J. Artif. Intell. Res.* 13 (2000), pp. 227–303. DOI: 10.1613/jair.639. URL: <https://doi.org/10.1613/jair.639>.
- [13] Zhuoru Li, Akshay Narayan, and Tze-Yun Leong. “An Efficient Approach to Model-Based Hierarchical Reinforcement Learning”. In: *Proceedings of the Thirty-First AAAI Conference on Artificial Intelligence, February 4-9, 2017, San Francisco, California, USA*. Ed. by Satinder P. Singh and Shaul Markovitch. AAAI Press, 2017, pp. 3583–3589. URL: <http://aaai.org/ocs/index.php/AAAI/AAAI17/paper/view/14771>.
- [14] Martin A. Riedmiller et al. “Learning by Playing Solving Sparse Reward Tasks from Scratch”. In: *Proceedings of the 35th International Conference on Machine Learning (ICML)*. Ed. by Jennifer G. Dy and Andreas Krause. Vol. 80. Proceedings of Machine Learning Research. PMLR, 2018, pp. 4341–4350. URL: <http://proceedings.mlr.press/v80/riedmiller18a.html>.

- [15] Carlos Florensa, Yan Duan, and Pieter Abbeel. “Stochastic Neural Networks for Hierarchical Reinforcement Learning”. In: *5th International Conference on Learning Representations, ICLR 2017, Toulon, France, April 24-26, 2017, Conference Track Proceedings*. OpenReview.net, 2017. URL: <https://openreview.net/forum?id=B1oK8aoxe>.
- [16] Peter Dayan and Geoffrey E. Hinton. “Feudal Reinforcement Learning”. In: *Advances in Neural Information Processing Systems 5, [NIPS Conference, Denver, Colorado, USA, November 30 - December 3, 1992]*. Ed. by Stephen Jose Hanson, Jack D. Cowan, and C. Lee Giles. Morgan Kaufmann, 1992, pp. 271–278. URL: <http://papers.nips.cc/paper/714-feudal-reinforcement-learning>.
- [17] Ofir Nachum et al. “Data-Efficient Hierarchical Reinforcement Learning”. In: *CoRR* abs/1805.08296 (2018). arXiv: 1805.08296. URL: <http://arxiv.org/abs/1805.08296>.
- [18] Andrew Levy et al. “Learning Multi-Level Hierarchies with Hindsight”. In: *7th International Conference on Learning Representations (ICLR)*. 2019. URL: <https://openreview.net/forum?id=ryzECoAcY7>.
- [19] Richard S. Sutton, Doina Precup, and Satinder P. Singh. “Between MDPs and Semi-MDPs: A Framework for Temporal Abstraction in Reinforcement Learning”. In: *Artif. Intell.* 112.1-2 (1999), pp. 181–211. DOI: 10.1016/S0004-3702(99)00052-1.
- [20] Pierre-Luc Bacon, Jean Harb, and Doina Precup. “The Option-Critic Architecture”. In: *CoRR* abs/1609.05140 (2016). arXiv: 1609.05140. URL: <http://arxiv.org/abs/1609.05140>.
- [21] Akhil Bagaria and George Konidaris. “Option Discovery using Deep Skill Chaining”. In: *8th International Conference on Learning Representations (ICLR)*. 2020. URL: <https://openreview.net/forum?id=B1gqipNYwH>.
- [22] Alexander C. Li et al. “Sub-policy Adaptation for Hierarchical Reinforcement Learning”. In: *8th International Conference on Learning Representations (ICLR)*. 2020. URL: <https://openreview.net/forum?id=ByeWogStDS>.
- [23] Jesse Zhang, Haonan Yu, and Wei Xu. “Hierarchical Reinforcement Learning By Discovering Intrinsic Options”. In: *International Conference on Learning Representations (ICLR)*. 2021.
- [24] George Konidaris, Leslie Pack Kaelbling, and Tomas Lozano-Perez. “From Skills to Symbols: Learning Symbolic Representations for Abstract High-Level Planning”. In: *J. Artif. Int. Res.* 61.1 (Jan. 2018), pp. 215–289. ISSN: 1076-9757.
- [25] Steven James, Benjamin Rosman, and George Konidaris. “Learning Portable Representations for High-Level Planning”. In: *Proceedings of the 37th International Conference on Machine Learning*. Ed. by Hal Daumé III and Aarti Singh. Vol. 119. Proceedings of Machine Learning Research. PMLR, 13–18 Jul 2020, pp. 4682–4691. URL: <https://proceedings.mlr.press/v119/james20a.html>.
- [26] Rodrigo Toro Icarte et al. “Learning Reward Machines for Partially Observable Reinforcement Learning”. In: *Advances in Neural Information Processing Systems*. Ed. by H. Wallach et al. Vol. 32. Curran Associates, Inc., 2019. URL: <https://proceedings.neurips.cc/paper/2019/file/532435c44bec236b471a47a88d63513d-Paper.pdf>.
- [27] Emre Ugur and Justus Piater. “Bottom-up learning of object categories, action effects and logical rules: From continuous manipulative exploration to symbolic planning”. In: *2015 IEEE International Conference on Robotics and Automation (ICRA)*. 2015, pp. 2627–2633. DOI: 10.1109/ICRA.2015.7139553.
- [28] Alper Ahmetoglu et al. “DeepSym: Deep Symbol Generation and Rule Learning from Unsupervised Continuous Robot Interaction for Planning”. In: *CoRR* abs/2012.02532 (2020). arXiv: 2012.02532. URL: <https://arxiv.org/abs/2012.02532>.
- [29] Masataro Asai and Alex Fukunaga. “Classical Planning in Deep Latent Space: Bridging the Subsymbolic-Symbolic Boundary”. In: *Proceedings of the Thirty-Second AAAI Conference on Artificial Intelligence, (AAAI-18), the 30th innovative Applications of Artificial Intelligence (IAAI-18), and the 8th AAAI Symposium on Educational Advances in Artificial Intelligence (EAAI-18), New Orleans, Louisiana, USA, February 2-7, 2018*. Ed. by Sheila A. McIlraith and Kilian Q. Weinberger. AAAI Press, 2018, pp. 6094–6101. URL: <https://www.aaai.org/ocs/index.php/AAAI/AAAI18/paper/view/16302>.

- [30] Tuomas Haarnoja et al. “Soft Actor-Critic: Off-Policy Maximum Entropy Deep Reinforcement Learning with a Stochastic Actor”. In: *Proceedings of the 35th International Conference on Machine Learning, ICML 2018, Stockholmsmässan, Stockholm, Sweden, July 10-15, 2018*. Ed. by Jennifer G. Dy and Andreas Krause. Vol. 80. Proceedings of Machine Learning Research. PMLR, 2018, pp. 1856–1865. URL: <http://proceedings.mlr.press/v80/haarnoja18b.html>.
- [31] Harold W Kuhn. “The Hungarian method for the assignment problem”. In: *Naval research logistics quarterly* 2.1-2 (1955), pp. 83–97.
- [32] James Munkres. “Algorithms for the assignment and transportation problems”. In: *Journal of the society for industrial and applied mathematics* 5.1 (1957), pp. 32–38.
- [33] Marcin Andrychowicz et al. “Hindsight Experience Replay”. In: *Advances in Neural Information Processing Systems 30: Annual Conference on Neural Information Processing Systems 2017, 4-9 December 2017, Long Beach, CA, USA*. Ed. by Isabelle Guyon et al. 2017, pp. 5048–5058. URL: <http://papers.nips.cc/paper/7090-hindsight-experience-replay>.
- [34] Sung Wook Yoon, Alan Fern, and Robert Givan. “FF-Replan: A Baseline for Probabilistic Planning”. In: *Proceedings of the Seventeenth International Conference on Automated Planning and Scheduling, ICAPS 2007, Providence, Rhode Island, USA, September 22-26, 2007*. Ed. by Mark S. Boddy, Maria Fox, and Sylvie Thiébaux. AAAI, 2007, p. 352. URL: <http://www.aaai.org/Library/ICAPS/2007/icaps07-045.php>.
- [35] Alexandre Campeau-Lecours et al. “Kinova Modular Robot Arms for Service Robotics Applications”. In: *Int. J. Robotics Appl. Technol.* 5.2 (2017), pp. 49–71. DOI: 10.4018/IJRAT.2017070104. URL: <https://doi.org/10.4018/IJRAT.2017070104>.

## S.1 Introduction

In the following we provide supplementary details and analysis of our approach. We show visualisations of the learned skills in Sec. S.2, give details on the robot experiment in sec. S.3 and provide additional details on ablations in sec. S.4. Architectural and implementation details are given in sec. S.5 for SEADS, in sec. S.6 for the SAC baseline and in sec. S.7 for the HAC baseline. In sec. S.8 we compare SEADS to the skill discovery method "Variational Intrinsic Control" (VIC, Gregor, Rezende, and Wierstra [1]). In Sec. S.9 we detail how we define training, validation and test splits on our proposed environments. Finally, we present detailed results for hyperparameter search on the SAC and HAC baselines in Sec. S.10.

## S.2 Learned skills

We provide visualizations on the behaviour of SEADS in Fig. S.5, showing that SEADS learns to assign skills to pushing individual fields on the game boards.

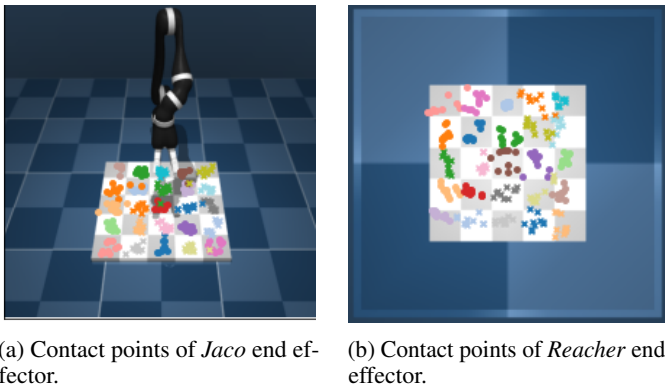


Figure S.5: Contact points of the *Jaco* (*Reacher*) end effector in the *LightsOutCursor* (*LightsOutReacher*) environments when executing skill  $k \in \{1, \dots, 25\}$  on 10 different initializations of the environment. Each skill is assigned a unique color/marker combination. We show the agent performance after  $1 \times 10^7$  environment steps. We observe that the SEADS agent learns to push individual fields as skills.

## S.3 Real Robot Experiment

For the real robot experiment we use a uArm Swift Pro robotic arm that interacts with a *LightsOut* board game. The board game runs on a Samsung Galaxy Tab A6 Android tablet with a screen size of 10.1 inches. We mapped the screen plane excluding the system status bar and action bar of the app (blue bar) to normalized coordinates  $(x, y) \in [0, 1]$ . A third  $z \in [0, 1]$  coordinate measures the perpendicular distance to the screen plane, with  $z = 1$  approximately corresponding to a distance of 10cm to the screen. To control the robot arm, we use the Python SDK from [2], which allows to steer the end effector to  $\vec{X} = (X, Y, Z)$  target locations in a coordinate frame relative to the robot's base. As the robot's base is not perfectly aligned with the tablet's surface, e.g. due to the rear camera, we employed a calibration procedure. We measured the location of the four screen corners in  $(X, Y, Z)$  coordinates using the SDK's `get_position` method (by placing the end effector holding the capacitive pen on the particular corners) and fitted a plane to these points minimizing the squared distance. We reproject the measured points onto the plane and compute a perspective transform by pairing the reprojected points with normalized coordinates  $(x, y) \in \{0, 1\} \times \{0, 1\}$ . To obtain robot coordinates  $(X, Y, Z)$  from normalized coordinates  $(x, y, z)$  we first apply the perspective transform on  $(x, y)$ , yielding  $\hat{X} = (X, Y, Z = 0)$ . We subsequently add the plane's normal to  $(X, Y, Z)$  scaled by  $z$  and an additional factor which controls the distance to the tablet's surface for  $z = 1$ .

The skill policy of SEADS outputs a normalized pushing coordinate  $(x, y) \in [0, 1]$  which is translated into a sequence of three commands sent to the robot, setting the position of the end effector to

$(x, y, z = 0.2)$ ,  $(x, y, z = 0)$ ,  $(x, y, z = 0.2)$  subsequently. The state of the board is communicated to the host machine running SEADS via USB through the logging functionality of the Android Debug Bridge. The whole system including robotic arm and Android tablet is interfaced as an OpenAI Gym [3] environment.

To simulate a more realistic gameplay, we do not resample the LightsOut board state or the robots’ pose at the beginning of an episode.

We show the setup and behaviour during training in Fig. S.6.

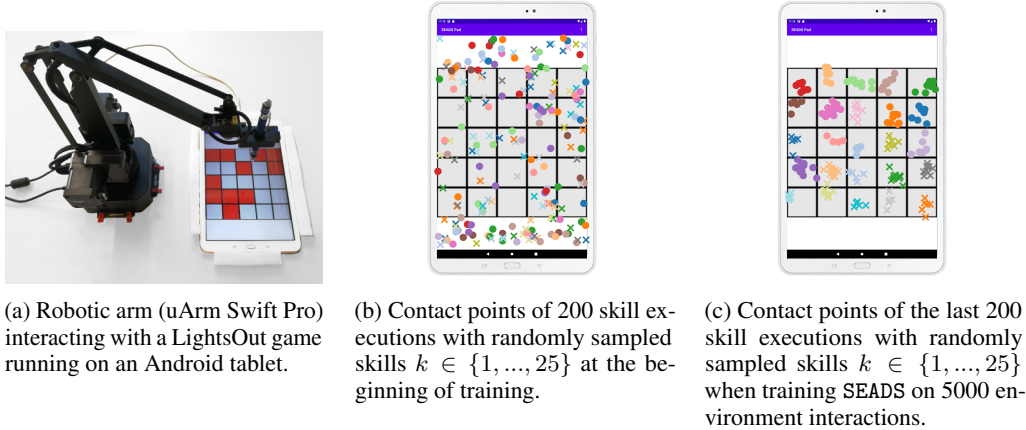


Figure S.6: Real-world setup with a robotic arm (a), on which SEADS learns a symbolic forward model on the LightsOut board state and associated low-level skills which relate to pushing locations on the tablet’s surface. In (b) and (c) we depict the first 200 and last 200 pushing locations of 5000 pushes used for training in total. While pushing locations are randomly scattered at the beginning of training (b), in the last 200 of 5000 training interactions skills relate to pushing particular fields on the game board (c).

## S.4 Extended ablation analysis

In this section we provide additional ablations for the episode relabelling and a quantitative analysis of the ablation experiments.

In addition to the “No relabelling” ablation considered in the main paper we investigate not relabelling episodes for training the SAC agent (No SAC relabelling) and not relabelling episodes for training the forward model (No forw. model relabelling). All evaluations are performed on 10 individually trained agents. We refer to Fig. S.7 for a visualization of the results. The results demonstrate that both relabelling for SAC training and for forward model training is important for the performance of SEADS.

In Table S.1 we present the number of average unique game moves executed as skills by SEADS and its ablations. On the simpler Cursor environments, most ablations perform similarly well as SEADS in finding almost all skills. The “No relabelling” ablation shows a drop in performance. On LightsOutReacher, most ablated design choices are important for the high performance of SEADS, while not performing second-best normalization achieves slightly better results than SEADS (+0.02 mean performance). On TileSwapReacher and the Jaco environments, SEADS performs better than all ablations.

We also observe that the “More skills” variant yields a slightly higher number of executed unique game moves in nearly all environments except TileSwapJaco, which is an encouraging result, justifying to over-estimate the number of skills  $K$  in situations where it is unknown.

## S.5 SEADS details

In the following, we will present algorithmic and architectural details of our approach.

	Cursor		Reacher		Jaco	
	LightsOut	TileSwap	LightsOut	TileSwap	LightsOut	TileSwap
SEADS	24.9 ± 0.1	11.92 ± 0.2	23.38 ± 0.93	11.54 ± 0.26	22.36 ± 1.4	11.36 ± 0.36
No sec.-best norm.	24.88 ± 0.29	11.82 ± 0.26	<u>23.4 ± 0.78</u>	11.44 ± 0.42	20.45 ± 2.14	<b>10.48 ± 1.03</b>
No nov. bonus	24.96 ± 0.06	11.87 ± 0.23	21.7 ± 1.02	11.21 ± 0.65	18.29 ± 1.75	10.8 ± 0.81
No relabelling	<b>24.52 ± 0.54</b>	<b>11.48 ± 0.53</b>	<b>17.03 ± 4.18</b>	<b>3.1 ± 2.05</b>	20.72 ± 0.84	10.8 ± 0.41
No forw. model rel.	24.96 ± 0.08	11.97 ± 0.03	20.6 ± 1.76	5.52 ± 4.03	18.16 ± 2.37	10.88 ± 0.8
No SAC relabelling	24.9 ± 0.07	11.83 ± 0.24	19.9 ± 0.98	11.4 ± 0.35	<b>6.42 ± 4.48</b>	11.12 ± 0.42
More skills	24.92 ± 0.11	11.97 ± 0.04	23.55 ± 0.95	11.69 ± 0.29	22.77 ± 1.0	11.33 ± 0.14

Table S.1: Number of average unique game moves executed as skills by SEADS and its ablations after training on  $5 \times 10^5$  (*Cursor*) /  $1 \times 10^7$  (*Reacher*, *Jaco*) environment interactions. Best performance on each environment is marked by underline, worst in red. The ablated design choices contribute to the performance of SEADS especially on the more difficult *Reacher* and *Jaco* environments. Overestimating the number of skills does not decrease performance (“More skills”). We show mean and standard deviation over 10 individually trained agents per ablation/environment.

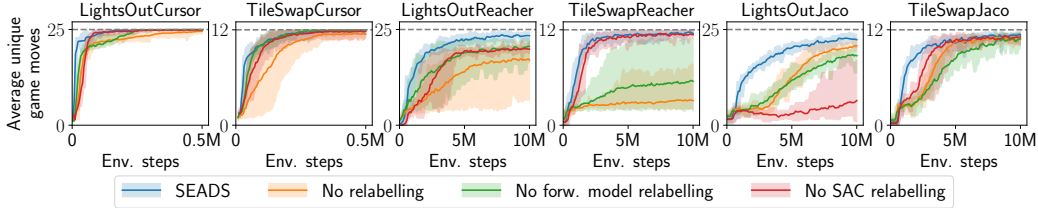


Figure S.7: Extended ablation analysis with additional relabelling ablations. The results demonstrate that both relabelling for SAC training and for forward model training is important for the performance of SEADS. See sec. S.4 for details.

### S.5.1 Task solution with and without replanning

One main idea of the proposed SEADS agent is to use separate phases of symbolic planning (using the symbolic forward model  $q_\theta(z_T | z_0, k)$ ) and low-level control (using the skill policies  $\pi(a | s, k)$ ) for solving tasks. In algorithm 1 and algorithm 2 we present pseudocode of task solution using planning and skill execution, with and without intermittent replanning.

### S.5.2 Training procedure

The main training loop of our proposed SEADS agent consists of intermittent episode collection and re-labelling for training the skill-conditioned policy  $\pi$  using soft actor-critic (SAC, [4]) and symbolic forward model (see Algorithm 3). For episode collection we first sample a skill from a uniform distribution over skills  $k \sim \text{Uniform}\{1, \dots, K\}$  and then collect the corresponding episode.

---

**Algorithm 1** Task solution (without replanning). `bfs_plan` denotes breadth-first search over a sequence of skills to transition  $z_{(0)}$  to  $z^*$ , leveraging the symbolic forward model  $q_\theta$ . Nodes are expanded in BFS via the function  $\text{successor}_{q_\theta} : \mathcal{Z} \times \mathcal{K} \rightarrow \mathcal{Z}$ .

---

**Input:** environment  $E$ , skill-conditioned policy  $\pi$ , symbolic forward model  $q_\theta$ , initial state  $s_{(0)} = s_0$ , symbolic goal  $z^*$ , symbolic mapping function  $\Phi$

**Output:** boolean success

$N, [k_1, \dots, k_N] = \text{bfs\_plan}(q_\theta, z_{(0)} = \Phi(s_{(0)}), z^*)$

**for**  $n = 1$  **to**  $N$  **do**

$s_{(n)} = \text{apply}(E, \pi, s_{(n-1)}, k_i)$

**end for**

success =  $(\Phi(s_{(N)}) == z^*)$

---

---

**Algorithm 2** Task solution (with replanning). `bfs_plan` denotes breadth-first search over a sequence of skills to transition  $z_{(0)}$  to  $z^*$ , leveraging the symbolic forward model  $q_\theta$ . Nodes are expanded in BFS via the function `successor $_{q_\theta}$`  :  $\mathcal{Z} \times \mathcal{K} \rightarrow \mathcal{Z}$ .

---

**Input:** environment  $E$ , skill-conditioned policy  $\pi$ , symbolic forward model  $q_\theta$ , initial state  $s_{(0)} = s_0$ , symbolic goal  $z^*$ , symbolic mapping function  $\Phi$   
 $n \leftarrow 0$   
**repeat**  
 $N, [k_1, \dots, k_N] \leftarrow \text{bfs\_plan}(q_\theta, z_{(n)} = \Phi(s_{(n)}), z^*)$   
**for**  $i \in \{1, \dots, N\}$  **do**  
 $n \leftarrow n + 1$   
 $\hat{z}_{(n)} \leftarrow \text{successor}_{q_\theta}(\Phi(s_{(n-1)}), k_i)$  {Compute the expected symbolic state after applying skill  $k_i$ }  
 $s_{(n)} \leftarrow \text{apply}(E, \pi, s_{(n-1)}, k_i)$   
 $z_{(n)} \leftarrow \Phi(s_{(n)})$   
**if**  $z_{(n)} \neq \hat{z}_{(n)}$  **then**  
**Break** {If the actual symbolic state differs from the predicted state, we replan}  
**end if**  
**end for**  
**until**  $z_{(n)} == z^*$

---

In our experiments we collect 32 episodes per epoch (i.e.,  $N_{\text{episodes}} = 32$ ) for the simulation experiments and 4 episodes per epoch for the robot experiment. We maintain two replay buffers of episodes for short-term (`Episodes $_{\text{recent}}$` ) and long-term storage (`Episodes $_{\text{buffer}}$` ), in which we keep the  $N_{\text{buffer}} = 2048 / N_{\text{recent}} = 256$  most recent episodes. For training the SAC agent and skill model we combine a sample of 256 episodes from the long-term buffer and all 256 episodes from the short-term buffer, comprising the episodes `Episodes`. These episodes are subsequently passed to the relabelling module. On these relabelled episodes the SAC agent and skill model are trained. Please see the following subsections for details on episode collection, relabelling, skill model training and policy training.

---

**Algorithm 3** SEADS training loop

---

**Input:** Environment  $E$   
Number of epochs  $N_{\text{epochs}}$   
Number of new episodes per epoch  $N_{\text{episodes}}$   
Episode buffer size  $N_{\text{buffer}}$   
**Result:** Trained skill-conditioned policy  $\pi(a | s, k)$  and forward model  $q_\theta(z_T | z_0, k)$   
`Episodes $_{\text{buffer}}$`  = [], `Episodes $_{\text{recent}}$`  = []  
**for**  $n_{\text{epoch}} = 1$  **to**  $N_{\text{epochs}}$  **do**  
**for**  $n_{\text{episode}} = 1$  **to**  $N_{\text{episodes}}$  **do**  
Sample  $k \sim p(k)$   
 $s_0 = E.\text{reset}()$   
 $\text{Ep} = \text{collect\_episode}(E, \pi, s_0, k)$   
`Episodes $_{\text{buffer}}$` .append( $\text{Ep}$ ), `Episodes $_{\text{recent}}$` .append( $\text{Ep}$ )  
**end for**  
`Episodes $_{\text{buffer}}$`   $\leftarrow$  `Episodes $_{\text{buffer}}$` [- $N_{\text{buffer}}$ :] {Keep  $N_{\text{buffer}}$  most recent episodes}  
`Episodes $_{\text{recent}}$`   $\leftarrow$  `Episodes $_{\text{recent}}$` [- $N_{\text{recent}}$ :]  
`Episodes` = sample(`Episodes $_{\text{buffer}}$` ,  $N = 256$ )  $\cup$  `Episodes $_{\text{recent}}$`   
`Episodes $_{\text{SM}}$`   $\leftarrow$  relabel(`Episodes`,  $p = 1.0$ )  
update\_skill\_model(`Episodes $_{\text{SM}}$` )  
`Episodes` = sample(`Episodes $_{\text{buffer}}$` ,  $N = 256$ )  $\cup$  `Episodes $_{\text{recent}}$`   
`Episodes $_{\text{SAC}}$`   $\leftarrow$  relabel(`Episodes`,  $p = 0.5$ )  
update\_sac(`Episodes $_{\text{SAC}}$` )  
**end for**

---

### S.5.2.1 Episode collection (collect\_episode)

The operator `collect_episode` works similar to the `apply` operator defined in the main paper (see sec. 3). It applies the skill policy  $\pi(a_t | s_t, k)$  iteratively until termination. However, the operator returns all intermediate states  $s_0, \dots, s_T$  and actions  $a_0, \dots, a_{T-1}$  to be stored in the episode replay buffers.

### S.5.2.2 Relabelling (relabel)

For relabelling we sample a Bernoulli variable with success probability of  $p$  for each episode in the Episodes buffer, indicating whether it may be relabeled. For training the forward model we potentially relabel all episodes ( $p = 1$ ), while for the SAC agent we only allow half of the episodes to be relabeled ( $p = 0.5$ ). The idea is to train the SAC agent also on *negative* examples of skill executions with small rewards. Episodes in which the symbolic observation did not change are excluded from relabelling. All episodes which should be relabeled are passed to the relabelling module as described in sec. 3. The union of these relabelled episodes and the episodes which were not relabeled form the updated buffer which is returned by the `relabel` operator.

### S.5.2.3 SAC agent update (update\_sac)

In each epoch, we fill a transition buffer using all transitions from the episodes in the `EpisodesSAC` buffer. Each transition tuple is of the form  $([s_t^i, k^i], a_t^i, [s_{t+1}^i, k^i], r_{t+1}^i)$  where  $s$  are environment observations,  $a$  low-level actions,  $k$  a one-hot representation of the skill and  $r$  the intrinsic reward.  $[\cdot]$  denotes the concatenation operation. The low-level SAC agent is trained for 16 steps per epoch on batches comprising 128 randomly sampled transitions from the transition buffer. We train the actor and critic networks using Adam [5]. For architectural details of the SAC agent, see sec. S.5.3.1.

### S.5.2.4 Skill model update (update\_skill\_model)

From the episode buffer `EpisodesSM` we sample transition tuples  $(z_0^i, k_i, z_{T^i}^i)$ . The skill model is trained to minimize an expected loss

$$\mathcal{L} = \mathbb{E}_{\mathcal{B}} \left[ \sum_{i \in \mathcal{B}} L(z_0^i, k_i, z_{T^i}^i) \right] \quad (2)$$

for randomly sampled batches  $\mathcal{B}$  of transition tuples. We optimize the skill model parameters  $\theta$  using the Adam [5] optimizer for 4 steps per epoch on batches of size 32. We use a learning rate of  $1 \cdot 10^{-3}$ . The instance-wise loss  $L$  to be minimized corresponds to the negative log-likelihood  $L = -\log q_{\theta}(z_{T^i}^i | z_0^i, k)$  for symbolic forward models or  $L = -\log q_{\theta}(k | z_0^i, z_{T^i}^i)$  for the VIC ablation (see sec. S.8).

## S.5.3 Architectural details

### S.5.3.1 SAC agent

We use the soft actor-critic implementation by Tandon [6] in our SEADS agent. Policy and critic networks are modeled by a multilayer perceptron with two hidden layers with ReLU activations. For hyperparameters, please see the table below.

<code>{LightsOut, TileSwap}</code> -	<i>Cursor</i>	<i>Reacher</i>	<i>Jaco</i>	Robot (LightsOut)
Learning rate	$3 \cdot 10^{-4}$	$3 \cdot 10^{-4}$	$3 \cdot 10^{-4}$	$3 \cdot 10^{-4}$
Target smoothing coeff. $\tau$	0.005	0.005	0.005	0.005
Discount factor $\gamma$	0.99	0.99	0.99	0.99
Hidden dim.	512	512	512	512
Entropy target $\alpha$	0.1	0.01	0.01	0.1
Automatic entropy tuning	no	no	no	no
Distribution over actions	Gaussian	Gaussian	Gaussian	Gaussian

### S.5.3.2 Symbolic forward model

Our symbolic forward model models the distribution over the terminal symbolic observation  $z_T$  given the initial symbolic observation  $z_0$  and skill  $k$ . It factorizes over the symbolic observation as



$q_\theta(z_T | k, z_0) = \prod_{d=1}^D q_\theta([z_T]_d | k, z_0) = \prod_{d=1}^D \text{Bernoulli}([\alpha_T(z_0, k)]_d)$  where  $D$  is the dimensionality of the symbolic observation. We assume  $z \in \mathcal{Z}$  to be a binary vector with  $\mathcal{Z} = \{0, 1\}^D$ . The Bernoulli probabilities  $\alpha_T(z_0, k)$  are predicted by a learnable neural component. We use a neural network  $f$  to parameterize the probability of the binary state in  $z_0$  to flip  $p_{\text{flip}} = f_\theta(z_0, k)$ , which simplifies learning if the *change* in symbolic state only depends on  $k$  and is independent of the current state. Let  $\alpha_T$  be the probability for the binary state to be True, then  $\alpha_T = (1 - z_0) \cdot p_{\text{flip}} + z_0 \cdot (1 - p_{\text{flip}})$ . The input to the neural network is the concatenation  $[z_0, \text{onehot}(k)]$ . We use a multilayer perceptron with two hidden layers with ReLU nonlinearities and 256 hidden units.

## S.6 SAC baseline

We train the SAC baseline in a task-specific way by giving a reward of 1 to the agent if the board state has reached its target configuration and 0 otherwise. At the beginning of each episode we first sample the difficulty of the current episode which corresponds to the number of moves required to solve the game (solution depth  $S$ ). For all environments  $S$  is uniformly sampled from  $\{1, \dots, 5\}$ . For all *Cursor* environments we impose a step limit  $T_{\text{lim}} = 10 \cdot S$ , for *Reacher* and *Jaco*  $T_{\text{lim}} = 50 \cdot S$ . This corresponds to the number of steps a single skill can make in SEADS multiplied by  $S$ . We use a replay buffer which holds the most recent 1 million transitions and train the agent with a batchsize of 256. The remaining hyperparameters (see table below) are identical to the SAC component in SEADS; except for an increased number of hidden units and an additional hidden layer (i.e., three hidden layers) in the actor and critic networks to account for the planning the policy has to perform. In each epoch of training we collect 8 samples from each environment which we store in the replay buffer. We performed a hyperparameter search on the number of agent updates performed in each epoch  $N$  and entropy target values  $\alpha$ . We also experimented with skipping updates, i.e., collecting 16 (for  $N = 0.5$ ) or 32 (for  $N = 0.25$ ) environment samples before performing a single update. We found that performing too many updates leads to unstable training (e.g.,  $N = 4$  for *LightsOutCursor*). For all results and optimal settings per environment, we refer to sec. S.10.1. For the SAC baseline we use the same SAC implementation [6] which we use for SEADS.

<i>{LightsOut, TileSwap}</i> -	<i>Cursor</i>	<i>Reacher</i>	<i>Jaco</i>
Learning rate	$3 \cdot 10^{-4}$	$3 \cdot 10^{-4}$	$3 \cdot 10^{-4}$
Target smoothing coeff. $\tau$	0.005	0.005	0.005
Discount factor $\gamma$	0.99	0.99	0.99
Hidden dim.	512	512	512
Entropy target $\alpha$	<i>tuned</i> (see sec. S.10.1)		
Automatic entropy tuning	no	no	no
Distribution over actions	Gaussian	Gaussian	Gaussian

## S.7 HAC baseline

For the HAC baseline we adapt the official code release by Levy [7]. We modify the architecture to allow for a two-layer hierarchy of policies in which the higher-level policy commands the lower-level policy with *discrete* subgoals (which correspond to the symbolic observations  $z$  in our case). This requires the higher-level policy to act on a discrete action space  $\mathcal{A}_{\text{high}} = \mathcal{Z}$ . The lower-level policy acts on the continuous actions space  $\mathcal{A}_{\text{low}} = \mathcal{A}$  of the respective manipulator (*Cursor*, *Reacher*, *Jaco*). To this end, we use a discrete-action SAC agent for the higher-level policy and a continuous-action SAC agent for the lower-level policy. For the higher-level discrete SAC agent we parameterize the distribution over actions as a factorized reparametrizable RelaxedBernoulli distribution, which is a special case of the Concrete [8] / Gumbel-Softmax [9] distribution. We use the implementation of [6] for the SAC agent on both levels and extend it by a RelaxedBernoulli distribution over actions for the higher-level policy.

### S.7.1 Hyperparameter search

We performed an extensive hyperparameter search on all 6 environments (*{LightsOut, TileSwap}*  $\times$  *{Cursor, Reacher, Jaco}*) for the HAC baseline. We investigated a base set of entropy target values  $\alpha_{\text{low}}, \alpha_{\text{high}} \in \{0.1, 0.01, 0.001, 0.0001\}$  for both layers separately. On the *Cursor* environments

we refined these sets in regions of high success rates. We performed a hyperparameter search on the temperature parameter  $\tau$  of the RelaxedBernoulli distribution on the *Cursor* environments with  $\tau \in \{0.01, 0.05, 0.1, 0.5\}$  and found  $\tau = 0.1$  to yield the best results. For experiments on the *Reacher* and *Jaco* environments we then fixed the parameter  $\tau = 0.1$ . We report results on parameter sets with highest average success rate on 5 individually trained agents after  $5 \times 10^5$  (*Cursor*) /  $1 \times 10^7$  (*Reacher*, *Jaco*) environment interactions. We refer to sec. S.10.2 for a visualization of all hyperparameter search results.

### Parameters for high-level policy

<i>all environments</i>	
Learning rate	$3 \cdot 10^{-4}$
Target smoothing coeff. $\tau$	0.005
Discount factor $\gamma$	0.99
Hidden layers for actor/critic	2
Hidden dim.	512
Entropy target $\alpha_{\text{high}}$	<i>tuned</i> (see sec. S.10.2)
Automatic entropy tuning	no
Distribution over actions	RelaxedBernoulli
RelaxedBernoulli temperature $\tau$	<i>tuned</i> (see sec. S.10.2)

### Parameters for low-level policy

<i>all environments</i>	
Learning rate	$3 \cdot 10^{-4}$
Target smoothing coeff. $\tau$	0.005
Discount factor $\gamma$	0.99
Hidden layers for actor/critic	2
Hidden dim.	512
Entropy target $\alpha_{\text{high}}$	<i>tuned</i> (see sec. S.10.2)
Automatic entropy tuning	no
Distribution over actions	Gaussian

## S.8 VIC baseline

We compare to Variational Intrinsic Control (VIC, Gregor, Rezende, and Wierstra [1]) as a baseline method of unsupervised skill discovery. It is conceptually similar to our method as it aims to find skills such that the mutual information  $\mathcal{I}(s_T, k | s_0)$  between the skill termination state  $s_T$  and skill  $k$  is maximized given the skill initiation state  $s_0$ . To this end it jointly learns a skill policy  $\pi(s_t | a_t, k)$  and *skill discriminator*  $q_\theta(k | s_0, s_T)$ . We adopt this idea and pose a baseline to our approach in which we model  $q_\theta(k | z_0, z_T)$  *directly* with a neural network, instead of modelling  $q_\theta(k | z_0, z_T)$  indirectly through a forward model  $q_\theta(z_T | z_0, k)$ . The rest of the training process including its hyperparameters is identical to SEADS. We implement  $q_\theta(k | z_0, z_T)$  by a neural network which outputs the parameters of a categorical distribution and is trained by maximizing the log-likelihood  $\log q_\theta(k | z_0^i, z_{T^i}^i)$  on transition tuples  $(z_0^i, k_i, z_{T^i}^i)$  (see sec. S.5.2.4). We experimented with different variants of passing  $(z_0^i, z_{T^i}^i)$  to the network: (i) concatenation  $[z_0^i, z_{T^i}^i]$  and (ii) concatenation with XOR  $[z_0^i, z_{T^i}^i, z_0^i \text{ XOR } z_{T^i}^i]$ . We only found the latter to show success during training. The neural network model contains two hidden layers of size 256 with ReLU activations (similar to the forward model). We also evaluate variants of VIC which are extended by our proposed *relabelling scheme* and *second-best reward normalization*. In contrast to VIC, our SEADS agent discovers all possible game moves reliably, see Fig. S.8 for details. No VIC variant detects all possible game moves (25 for *LightsOut*, 12 for *TileSwap*) for the considered number of training environment interactions.

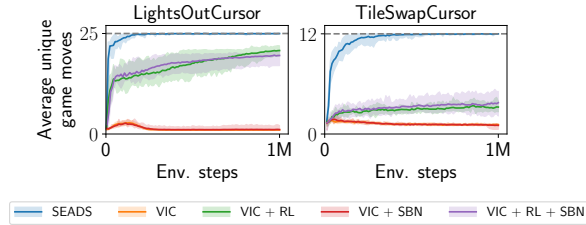


Figure S.8: Number of discovered skills on the `LightsOutCursor`, `TileSwapCursor` environments for the SEADS agent and variants of VIC [1]. Only SEADS discovers all skills reliably. See sec. S.8 for details.

For plain VIC and VIC extended by the second-best reward normalization (+*SBN*, sec. 3), a small progress in learning skills is observed at the beginning of training which decays quickly. Our proposed relabelling scheme (+*RL*, sec. 3) significantly improves the performance of VIC to learn distinct skills. Combining the second-best reward normalization and relabelling (*RL+SBN*) does not significantly improve performance over relabelling only (+*RL*).

## S.9 Environment details

### S.9.1 Training-/Validation-/Test-split

In order to ensure disjointness of board configurations in train, validation and test split we label each board configuration based on a hash remainder. For the hashing algorithm we first represent the current board configuration as comma-separated string, e.g.  $s = "1, 1, 0, \dots, 0"$  for `LightsOut` and  $s = "1, 0, 2, \dots, 8"$  for `TileSwap`. Then, this string is passed through a CRC32 hashing function, yielding the split based on an integer division remainder

$$\text{split} = \begin{cases} \text{train} & \text{CRC32}(s) \bmod 3 = 0 \\ \text{val} & \text{CRC32}(s) \bmod 3 = 1 \\ \text{test} & \text{CRC32}(s) \bmod 3 = 2 \end{cases} \quad (3)$$

### S.9.2 Board initialization

We quantify the difficulty of a particular board configuration by its *solution depth*, i.e., the minimal number of game moves required to solve the board.

For `LightsOut`, generating a board configuration for a given solution depth  $S$  can be achieved by pushing  $S$  *unique* fields on the initial all-lights-off board. Pushing a field twice reduces the solution depth.

For `TileSwap`, this simple rule does not hold. While there are cases where applying the "swap" operation to a pair of fields twice does reduce the solution depth, e.g. when swapping chips on the same pair of fields twice in a row, this does not hold for arbitrary situations where different swaps may have been performed in the meantime. Therefore we apply a different strategy to generate boards of a desired solution depth for `TileSwap`. First, we generate all possible sequences of swaps up to the desired solution depth  $S$  ( $12^S$  sequences for our  $3 \times 3$  `TileSwap`). Then, we simulate these swaps, and drop a swap sequence for the desired solution depth if a swap in the sequence effectively "undoes" a prior swap. We detect this "undo" operation by checking if a swap results in a field/chip-assignment which already exists in a previous board in the current sequence of swaps. This means that the current swap operation undoes a swap which has been performed on the previous board. For the remaining action sequences we check the actual solution depth of the configuration with breadth-first search. As this is a computationally complex procedure, we pre-compute all possible boards for solution depths up to 5 (the maximal solution depth used in this paper).

In table S.2 we show the sizes of the training, validation and test split for `LightsOut` and `TileSwap` environments for solution depths in  $\{1, \dots, 5\}$ .

		solution depth				
		1	2	3	4	5
LightsOut	train	7	99	785	4200	17849
	val	7	93	772	4268	17368
	test	11	108	743	4182	17913
	total	25	300	2300	12650	53130
TileSwap	train	7	31	179	683	2237
	val	5	19	154	628	2223
	test	0	38	137	667	2198
	total	12	88	470	1978	6658

Table S.2: Number of initial board configurations for varying solution depths and dataset splits (training / validation / test).

## S.10 Results of hyperparameter search on HAC and SAC baselines

### S.10.1 Results of SAC hyperparameter search

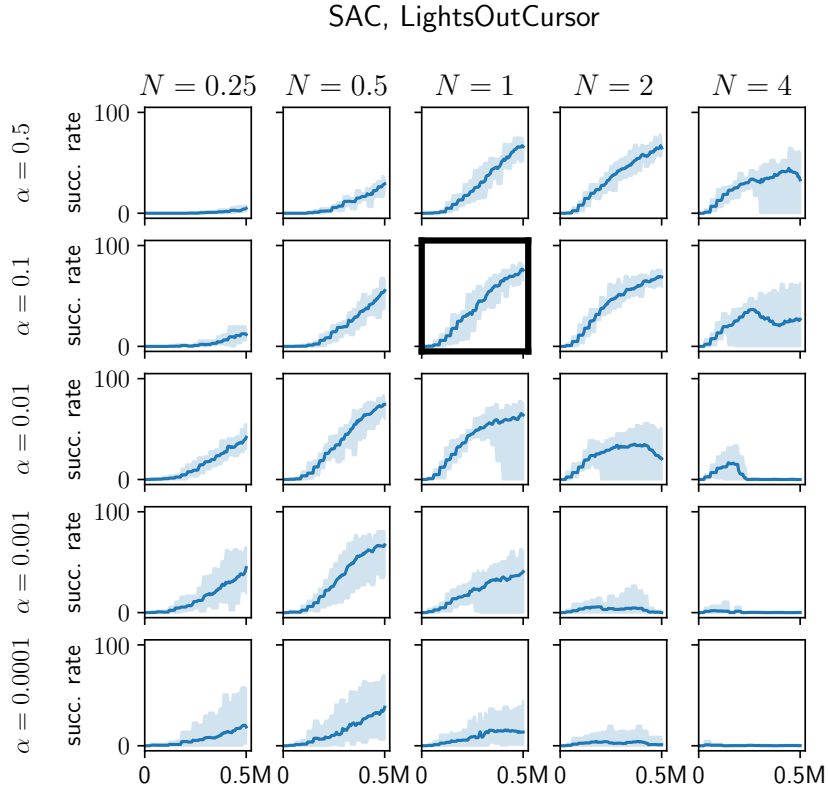


Figure S.9: Test performance of SAC agents on the LightsOutCursor environment for varying number of update steps per epoch ( $N$ ) and parameters  $\alpha$ . We evaluate 5 individual agents per configuration. The best configuration is marked in **bold** ( $N = 1, \alpha = 0.1$ ).

### SAC, TileSwapCursor

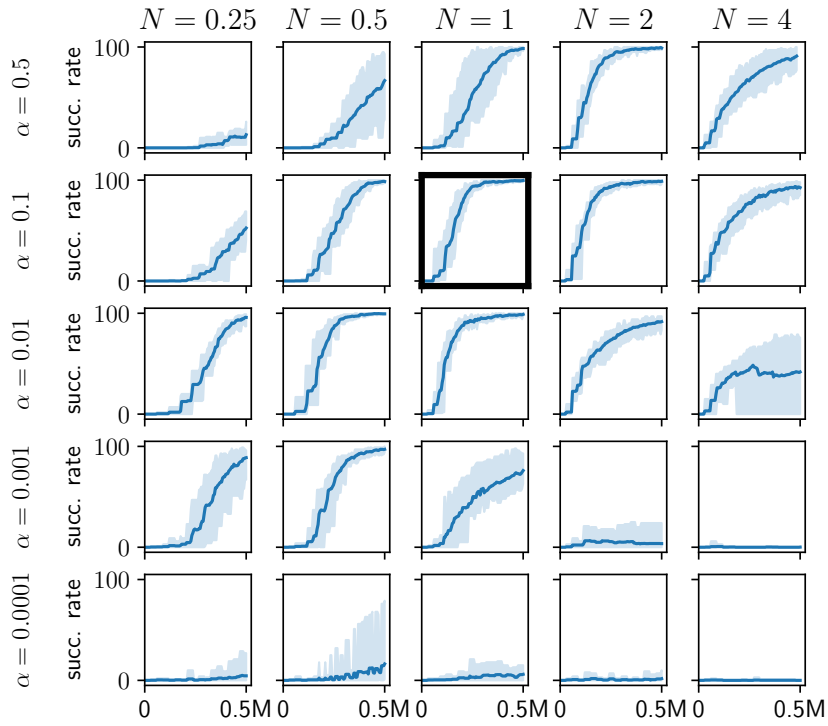


Figure S.10: Test performance of SAC agents on the TileSwapCursor environment for varying number of update steps per epoch ( $N$ ) and parameters  $\alpha$ . We evaluate 5 individual agents per configuration. The best configuration is marked in **bold** ( $N = 1, \alpha = 0.1$ ).

### SAC, LightsOutReacher

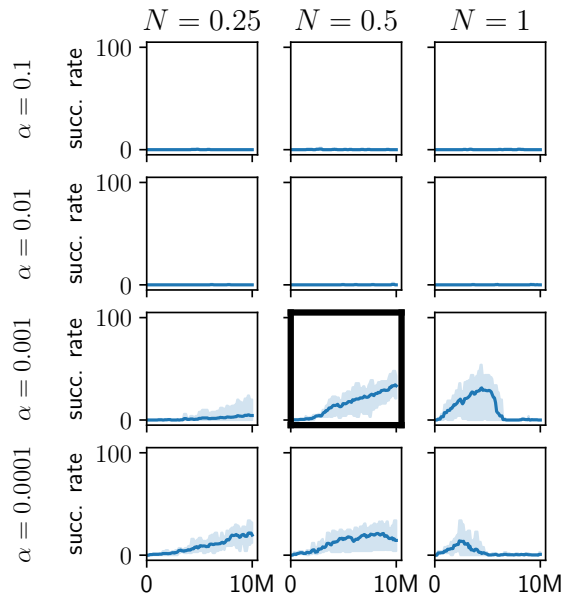


Figure S.11: Test performance of SAC agents on the LightsOutReacher environment for varying number of update steps per epoch ( $N$ ) and parameters  $\alpha$ . We evaluate 5 individual agents per configuration. The best configuration is marked in **bold** ( $N = 0.5, \alpha = 0.001$ ).

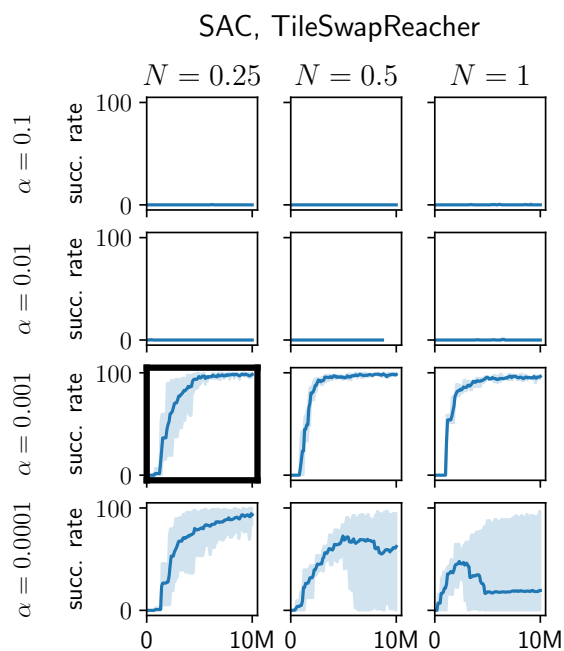


Figure S.12: Test performance of SAC agents on the TileSwapReacher environment for varying number of update steps per epoch ( $N$ ) and parameters  $\alpha$ . We evaluate 5 individual agents per configuration. The best configuration is marked in **bold** ( $N = 0.25$ ,  $\alpha = 0.001$ ).

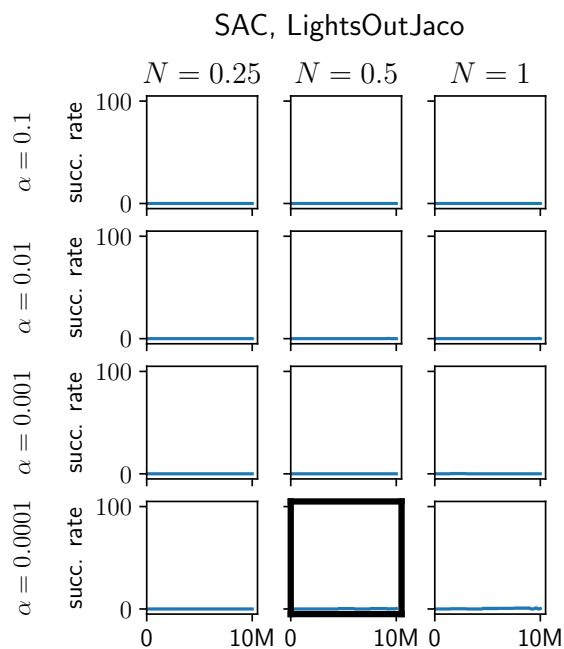


Figure S.13: Test performance of SAC agents on the LightsOutJaco environment for varying number of update steps per epoch ( $N$ ) and parameters  $\alpha$ . We evaluate 5 individual agents per configuration. The best configuration is marked in **bold** ( $N = 0.5$ ,  $\alpha = 0.0001$ ).

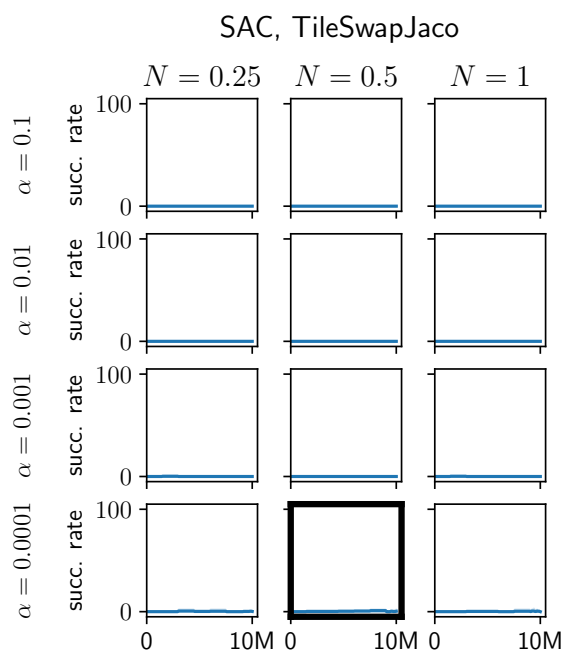
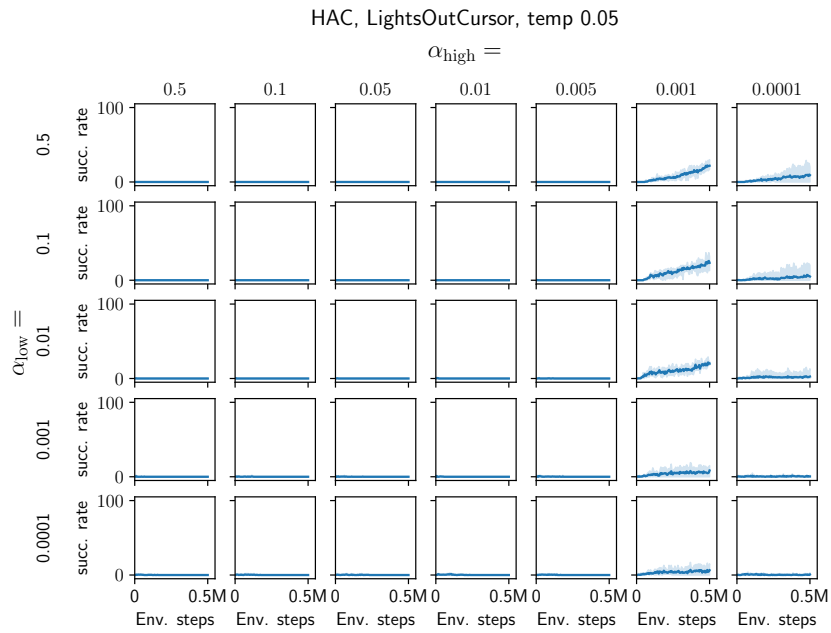
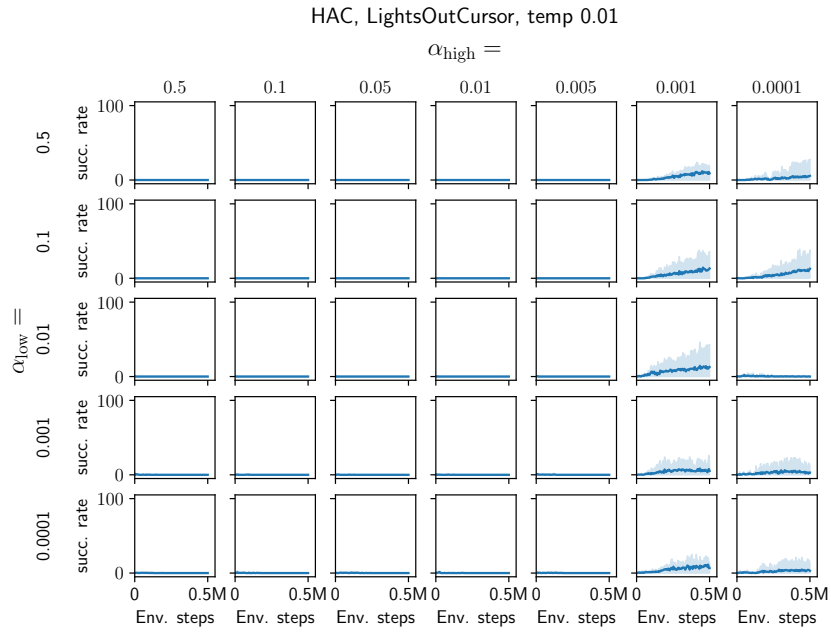


Figure S.14: Test performance of SAC agents on the TileSwapReacher environment for varying number of update steps per epoch ( $N$ ) and parameters  $\alpha$ . We evaluate 5 individual agents per configuration. The best configuration is marked in **bold** ( $N = 0.5, \alpha = 0.0001$ ).



## S.10.2 Results of HAC hyperparameter search



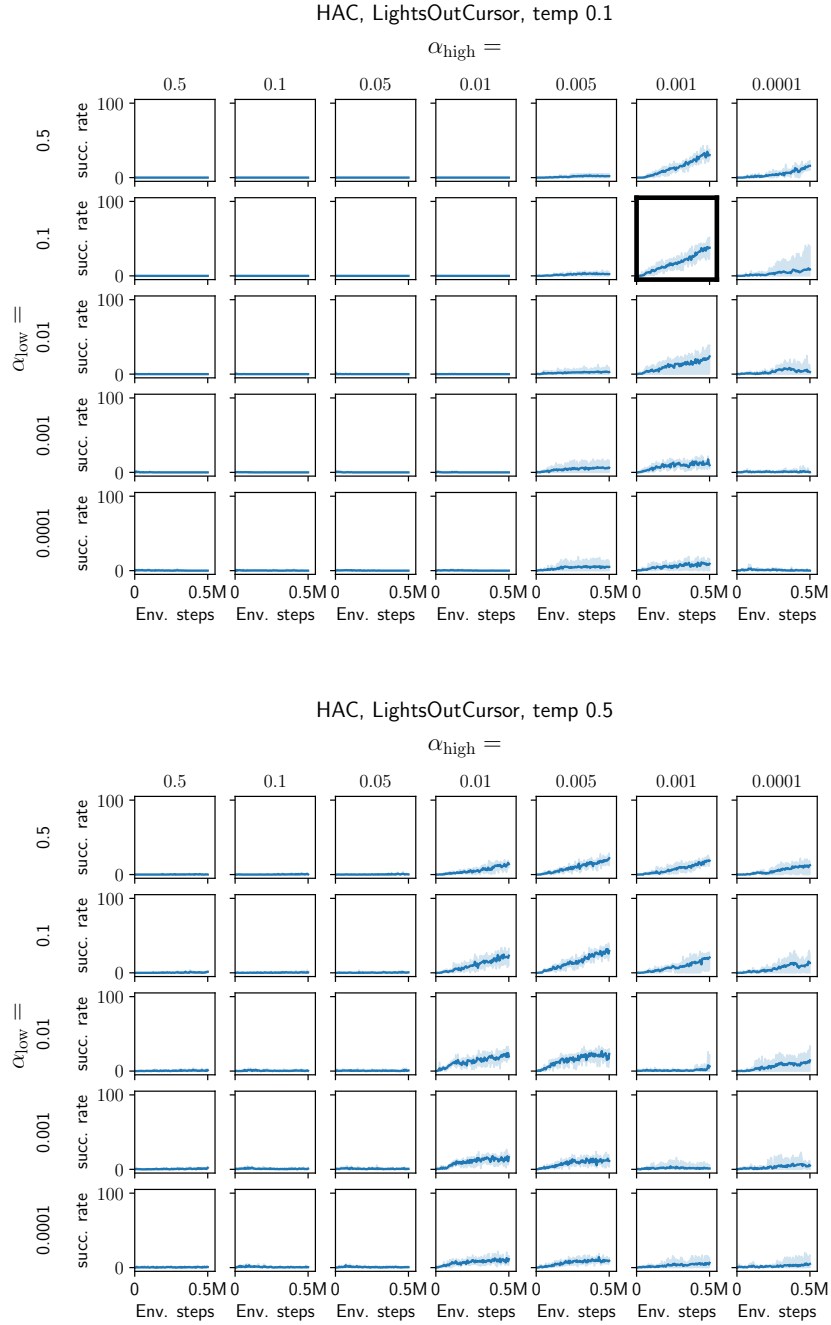
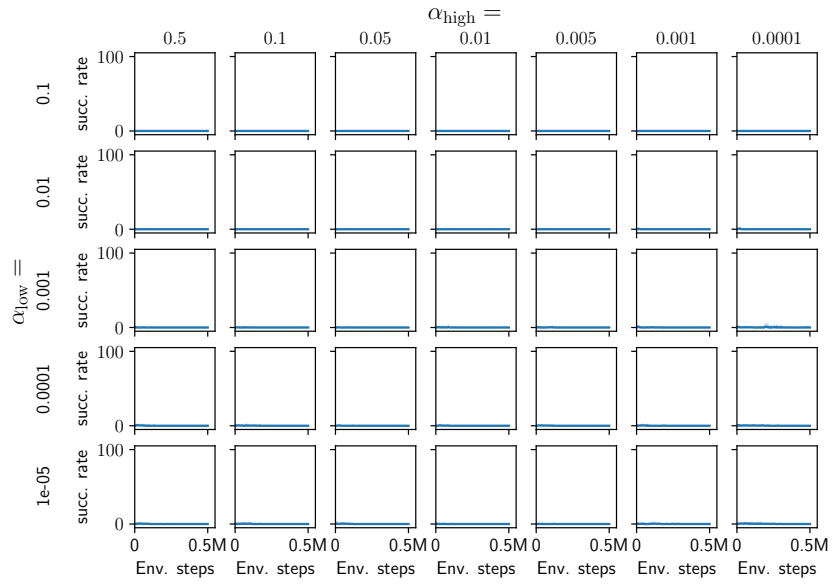
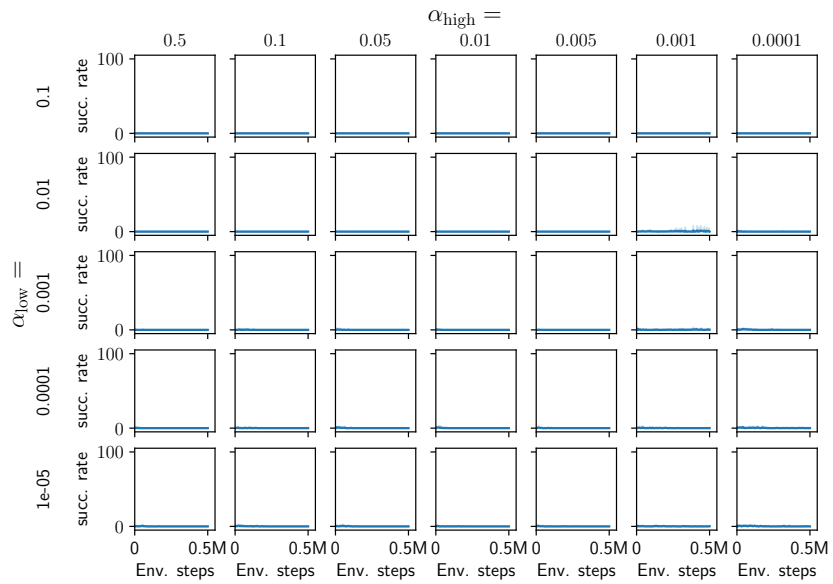


Figure S.14: Test performance of HAC agents on the LightsOutCursor environment for varying values for RelaxedBernoulli temperature  $\tau$  and entropy targets  $\alpha_{\text{high}}, \alpha_{\text{low}}$ . We evaluate 5 individual agents per configuration. The best configuration is marked in **bold** ( $\tau = 0.1, \alpha_{\text{low}} = 0.1, \alpha_{\text{high}} = 0.001$ ).

HAC, TileSwapCursor, temp 0.01



HAC, TileSwapCursor, temp 0.05



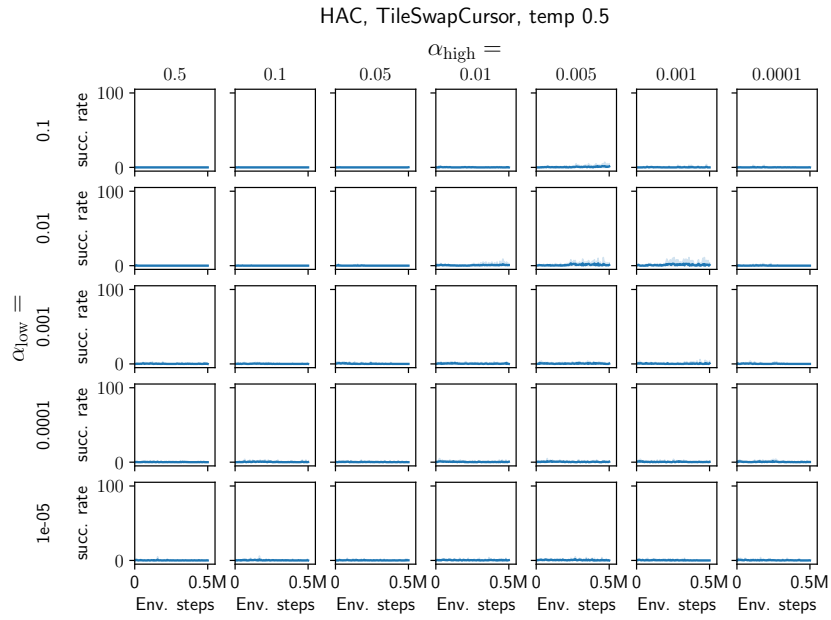
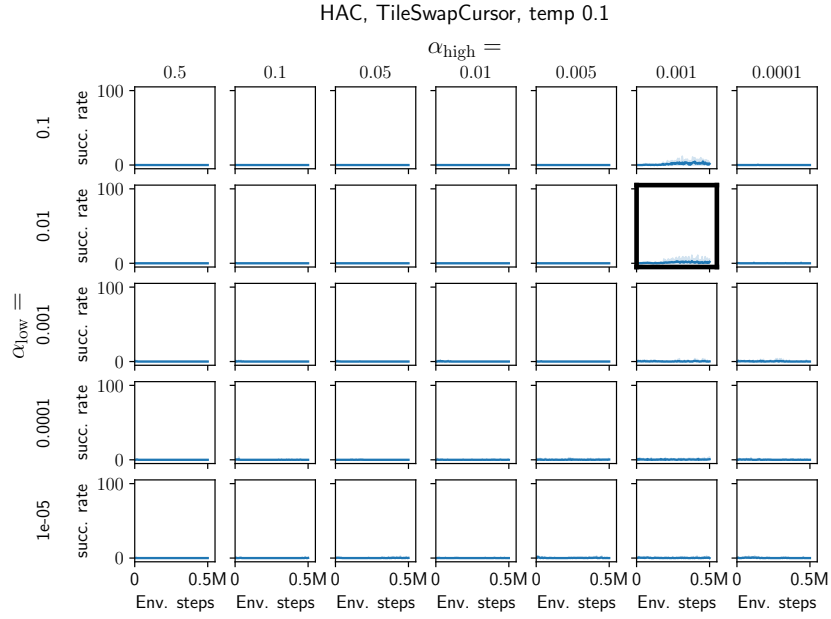


Figure S.14: Test performance of HAC agents on the TileSwapCursor environment for varying values for RelaxedBernoulli temperature  $\tau$  and entropy targets  $\alpha_{\text{high}}, \alpha_{\text{low}}$ . We evaluate 5 individual agents per configuration. The best configuration is marked in **bold** ( $\tau = 0.1, \alpha_{\text{low}} = 0.01, \alpha_{\text{high}} = 0.001$ ).

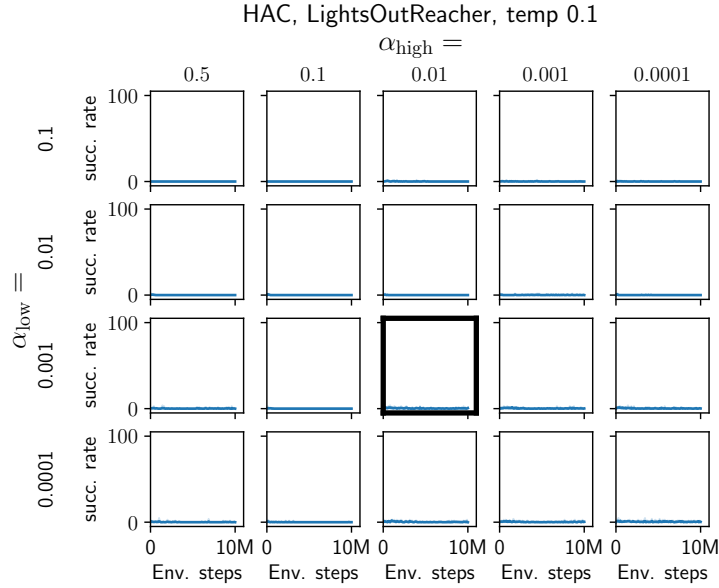


Figure S.15: Test performance of HAC agents on the `LightsOutReacher` environment for varying values for the entropy targets  $\alpha_{\text{high}}$ ,  $\alpha_{\text{low}}$  and fixed RelaxedBernoulli temperature  $\tau = 0.1$ . We evaluate 5 individual agents per configuration. The best configuration is marked in **bold** ( $\tau = 0.1$ ,  $\alpha_{\text{low}} = 0.001$ ,  $\alpha_{\text{high}} = 0.01$ ).

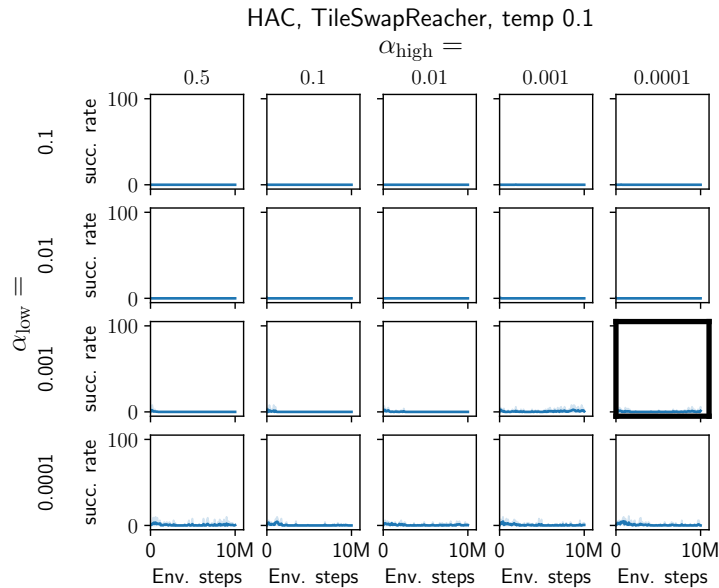


Figure S.16: Test performance of HAC agents on the `TileSwapReacher` environment for varying values for the entropy targets  $\alpha_{\text{high}}$ ,  $\alpha_{\text{low}}$  and fixed RelaxedBernoulli temperature  $\tau = 0.1$ . We evaluate 5 individual agents per configuration. The best configuration is marked in **bold** ( $\tau = 0.1$ ,  $\alpha_{\text{low}} = 0.001$ ,  $\alpha_{\text{high}} = 0.0001$ ).

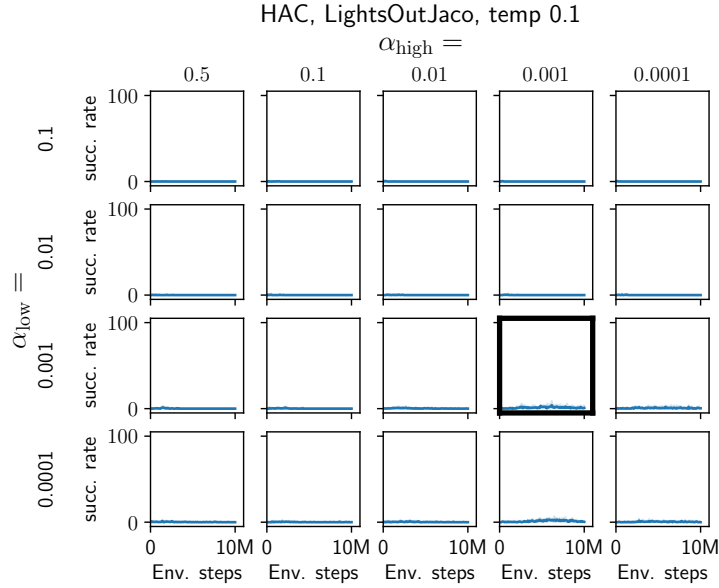


Figure S.17: Test performance of HAC agents on the LightsOutJaco environment for varying values for the entropy targets  $\alpha_{\text{high}}$ ,  $\alpha_{\text{low}}$  and fixed RelaxedBernoulli temperature  $\tau = 0.1$ . We evaluate 5 individual agents per configuration. The best configuration is marked in **bold** ( $\tau = 0.1$ ,  $\alpha_{\text{low}} = 0.001$ ,  $\alpha_{\text{high}} = 0.001$ ).

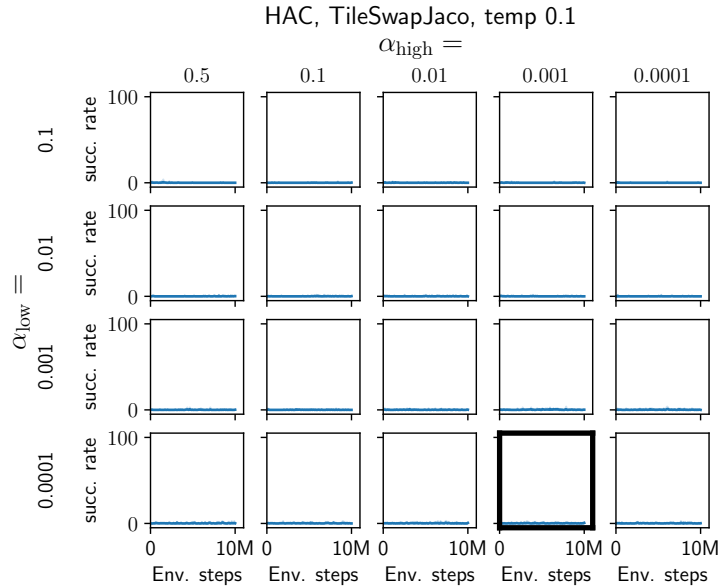


Figure S.18: Test performance of HAC agents on the TileSwapJaco environment for varying values for the entropy targets  $\alpha_{\text{high}}$ ,  $\alpha_{\text{low}}$  and fixed RelaxedBernoulli temperature  $\tau = 0.1$ . We evaluate 5 individual agents per configuration. The best configuration is marked in **bold** ( $\tau = 0.1$ ,  $\alpha_{\text{low}} = 0.0001$ ,  $\alpha_{\text{high}} = 0.001$ ).

## References

- [1] Karol Gregor, Danilo Jimenez Rezende, and Daan Wierstra. “Variational Intrinsic Control”. In: *International Conference on Learning Representations (ICLR), Workshop Track Proceedings*. OpenReview.net, 2017. URL: <https://openreview.net/forum?id=Skc-Fo4Yg>.
- [2] uArm-Developer. *uArm-Python-SDK*. <https://github.com/uArm-Developer/uArm-Python-SDK>. 2021.
- [3] Greg Brockman et al. *OpenAI Gym*. 2016. eprint: [arXiv:1606.01540](https://arxiv.org/abs/1606.01540).
- [4] Tuomas Haarnoja et al. “Soft Actor-Critic: Off-Policy Maximum Entropy Deep Reinforcement Learning with a Stochastic Actor”. In: *Proceedings of the 35th International Conference on Machine Learning, ICML 2018, Stockholmsmässan, Stockholm, Sweden, July 10-15, 2018*. Ed. by Jennifer G. Dy and Andreas Krause. Vol. 80. Proceedings of Machine Learning Research. PMLR, 2018, pp. 1856–1865. URL: <http://proceedings.mlr.press/v80/haarnoja18b.html>.
- [5] Diederik P. Kingma and Jimmy Ba. “Adam: A Method for Stochastic Optimization”. In: *3rd International Conference on Learning Representations, ICLR 2015, San Diego, CA, USA, May 7-9, 2015, Conference Track Proceedings*. 2015. URL: <http://arxiv.org/abs/1412.6980>.
- [6] Pranjali Tandon. *pytorch-soft-actor-critic*. <https://github.com/pranz24/pytorch-soft-actor-critic>. 2021.
- [7] Andrew Levy. *Hierarchical-Actor-Critic-HAC*. <https://github.com/andrew-j-levy/Hierarchical-Actor-Critic-HAC>. 2020.
- [8] Chris J. Maddison, Andriy Mnih, and Yee Whye Teh. “The Concrete Distribution: A Continuous Relaxation of Discrete Random Variables”. en. In: *arXiv:1611.00712 [cs, stat]* (Nov. 2016). arXiv: 1611.00712. URL: <http://arxiv.org/abs/1611.00712> (visited on 01/23/2019).
- [9] Eric Jang, Shixiang Gu, and Ben Poole. “Categorical Reparameterization with Gumbel-Softmax”. en. In: *arXiv:1611.01144 [cs, stat]* (Nov. 2016). arXiv: 1611.01144. URL: <http://arxiv.org/abs/1611.01144> (visited on 01/23/2019).